Department of Chemistry
Faculty of Science
University of Helsinki
Helsinki, Finland

Solution Properties and Self-Assembling of Cationic Diblock Copolymers

Vikram Baddam

DOCTORAL DISSERTATION

To be presented, with the permission of the Faculty of Science of the University of Helsinki, for public examination in Auditorium A110 of the Department of Chemistry, on August 26th 2022 at 12 o'clock noon.

Helsinki 2022

Supervisor

Professor Heikki Tenhu
Department of Chemistry
University of Helsinki
Finland

Opponent

Professor Mauri Kostiainen
Department of Bioproducts and Biosystems
School of Chemical Engineering
Aalto University
Finland

Reviewers

Professor Eva Malmström Jonsson
Department of Fibre and Polymer Technology
School of Engineering Sciences in Chemistry, Biotechnology and Health
KTH Royal institute of Technology
Sweden

&

Professor Jukka Seppälä
Department of Chemical and Metallurgical Engineering
School of Chemical Engineering
Aalto University
Finland

ISBN 978-951-51-8361-3 (softcover)
ISBN 978-951-51-8362-0 (PDF)

https://ethesis.helsinki.fi
Unigrafia
Helsinki 2022

Abstract

Solution properties and self-assembling of three polycations have been studied. The main emphasis was on poly((vinylbenzyl) trimethylammonium triflate) (PVBTMA-OTf), synthesized via RAFT polymerization. The PVBTMA-OTf is soluble in water, however, the presence of triflate ions turned it thermoresponsive. Both PVBTMA-OTf and its counterpart with a chloride counterion (PVBTMAC) underwent an UCST type phase transition in aqueous triflate solutions. With increasing the molar mass the cloud point shifted to higher temperatures. The behavior was different in two less hydrophobic polycations, poly((2-(methacryloyloxy)ethyl) trimethylammonium chloride) (PMOTAC) and poly (3-(acrylamidopropyl)trimethylammonium chloride) (PAMPTMAC). Higher amounts of hydrophobic ions were needed to induce the UCST behavior.

Diblock copolymers comprised of a poly(ethylene glycol) (PEG) block and PVBTMA-OTf with different block lengths were synthesized via controlled RAFT polymerizations. The block copolymers underwent stepwise phase separation when the polycation blocks were kept short. During cooling, the polymers first phase separated below cloud point temperature (T_{cU}), but solutions became clear (at T_{cL}) upon further cooling. The stepwise phase separation was dependent on the LiOTf concentration and molar mass of the polymers. The copolymers with longer cationic blocks phase separated in a single step similarly to the phase separation of the homopolymer PVBTMA-OTf. The block copolymers formed core-shell particles below T_{cL}. Copolymers with short cationic blocks built up PEG-stabilized particles, however, when the positively charged blocks were long, PEG was buried inside the particles. Due to the complex interactions between two blocks and as well as the interactions mediated by the counterions, the segregation of the blocks is difficult. As a result, with increasing the cationic block length the copolymers phase separated into complex aggregates.

Styrenic polycations PVBTMAC were chain extended with diacetone acrylamide (DAAM) via RAFT in aqueous solutions. Only spherical particles were obtained in pure water. However, by increasing the ionic ratio [NaCl]/[Cp] (where [Cp] is the concentration of cationic repeating unit), the particle morphology changed from spheres to fused aggregates or worms, even to vesicles when short styrenic macroCTAs were used. The final morphology was depended on the second block length and the solids content. Copolymers with either long styrenic stabilizers or with other macroCTAs, PMOTAC and PAMPTMAC formed spheres, cloudberries, or raspberries with increasing the salt concentration or the solids content.

Cationic particles from PVBTMAC prepared in salt-free dispersions phase separated in aqueous triflate solutions at a critical temperature. In some cases, the phase separation occurred in two steps. When the PISA reactions were conducted in triflate solutions, fused spheres were obtained. Increasing the solids content, particle morphologies evolved to vesicles with small lumens. The particles prepared at 70° C in aqueous LiOTf changed from spheres or fused spheres to wormlike networks/ fused aggregates when cooled to room temperature. On the other hand, the morphologies of the particles prepared with PMOTAC or PAMPTMAC macroCTAs were not affected by triflate ions.

To sum up, this work presents the use of triflate ions to induce thermoresponsive behavior in polycations and their diblock copolymers. Covalent linkage of hydrophilic PEG blocks to the responsive polycation PVBTMA-OTf enhances the stability of the particles, and the behavior is dependent on molar mass and LiOTf concentration. Using styrenic polycations as sole steric

stabilizers in PISA, a full morphological window of particles can be obtained simply by adjusting the ionic strength. The particles made with styrene based cationic stabilizers also show UCST behavior. This study demonstrates the use of triflate ions in PISA to induce order-order or morphological transitions.

Acknowledgements

This work was conducted in the polymer and colloids group at the Department of Chemistry, University of Helsinki, under supervision of Professor Heikki Tenhu during the years 2017-22. Center for international mobility (CIMO) and Magnus Ehrnrooth foundation are greatly acknowledged for the financial support of the studies. I also thank EMBI and ALD units for the electron microscope services, and CHEMS for the travel grants and seminars.

I am very grateful to my supervisor Professor Heikki Tenhu for his mentorship and guidance. This endeavor would not have been possible without his support, encouragement, and kindness. I admire his immense input and patience in my text editing. I am deeply indebted for his time spent helping me on many occasions and for the opportunities provided to me to grow in my professional life.

I also wish to thank Professor Jukka Seppälä and Professor Eva Malmström Jonsson for their time to review this dissertation and Professor Mauri Kostiainen for agreeing to be my opponent.

My sincere thanks to Dr. Sami Hietala for his kind assistance during these years. I am also grateful to Dr. Vladimir Aseyev for his readiness to speak about all kinds of matters. Big thanks goes to Dr. Erno Karjalainen for his scientific advices and from whose dissertation the current studies are developed. I am also grateful to Professor Sirkka-Liisa Maunu, the former leader of the group, to Dr. Sami-Pekka Hirvonen and Seija Lemettinen for their help and assistance. I thank Professor Robert Luxenhofer for paper beers and discussions. I would like to mention the late Professor Francoise Winnik for encouragement and discussions.

I thank all my collaborators Lauri Välinen, Linus Kuckling, Reetta Missonen, Kati Meriläinen, Nick Richert, and Elisa Spönla for their efforts in the synthesis and collection of the data. I have learned a lot while working with you all.

Many thanks to Joonas, Tony, and Satu for their friendly and scientific discussions. I appreciate Dong for his close friendship and helping nature. I take this opportunity to express my gratitude to all my dear current and former colleagues, Erasmus friends, polyhikers, office colleagues, and many others whom I met during the past years in the polymer lab. People who deserve special thanks are Tina, Fabian, Balázs, Jingwen, Oscar, Lauri M., Zeynab, Andrew, Larissa, Anna-Lena, Waqas, Juliane, Florian, Lando and many others. The colleagues outside the lab, Daniel, Sudeep, Eliza, and Andreas also deserve warmest thanks. I thank all for their warm friendship and for the fun times we had during the Christmas parties, HYPPY events, karaokes, lunches, travels, football/futsal, hiking, dinners, sauna, and tea times.

I am also thankful to friends from the Tampere group Harsha, Karunakar, and Vijender, and friends from the Tallinn group Chetan, Vinay, Anil, Naga, Modith, and Shiva for their moral support. I thank Victoria, Joan, Aino, and Gowtham for their friendship and care.

I express my deepest gratitude to my family and friends for their support and continuous encouragement. I also thank the Kuittinen family for their affection and good wishes. Finally, I owe my deepest gratitude to Elina for her care and love. I am very thankful for her immense support and understanding of me, even in my hard times.

Contents

List of original publications

This thesis is based on the following publications:

I. Baddam, V.; Aseyev, V.; Hietala, S.; Karjalainen, E.; Tenhu, H. **Polycation-PEG Block Copolymer Undergoes Stepwise Phase Separation in Aqueous Triflate Solution.** *Macromolecules* 2018, 51 (23), 9681–9691.

II. Baddam, V.; Missonen, R.; Hietala, S.; Tenhu, H. **Molecular Mass Affects the Phase Separation of Aqueous PEG–Polycation Block Copolymer.** *Macromolecules* 2019, 52 (17), 6514-6522.

III. Baddam, V.; Välinen, L.; Tenhu, H. **Thermoresponsive Polycation-Stabilized Nanoparticles through PISA. Control of Particle Morphology with a Salt.** *Macromolecules* 2021, 54 (9), 4288–4299.

IV. Baddam, V.; Välinen, L.; Kuckling, L.; Tenhu, H. **Morphological transitions of cationic PISA particles by salt, triflate ions and temperature; comparison of three polycations.** *Polym. Chem.* 2022, 13, 3790–3799.

The publications are referred to in the text by their roman numerals.

The author's contribution to the publications:

For all publications, the author designed the research plans and analyzed all the data. For publications I and II, the author conducted most of the syntheses and experimental work. For articles III and IV, the author planned all the syntheses and conducted major part of characterization works. The author wrote all the manuscripts and finalized them together with the coauthors.

List of abbreviations and symbols

[Cp]	Cationic repeating unit
[NaCl]/[Cp]	Ionic ratio
4VP	4-Vinylpyridine
ACVA	4,4′-Azobis(4-cyanovaleric acid)
AIBN	Azobis(isobutyronitrile)
AMPTAMC	(3-Acrylamidopropyl)trimethylammonium chloride
ATRP	Atom transfer radical polymerization
BF_4^-	Tetrafluoroborate
CCTPA	4-((((2-Carboxyethyl)thio)carbonothioyl)thio)-4-cyanopentanoic acid
CPDTC	2-Cyano-2-propyldodecyltrithiocarbonate
CRP	Controlled radical polymerization
CTA	Chain transfer agent
CTPA	2-(2-Carboxyethylsulfanylthiocarbonylsulfanyl) propionic acid
DAAM	Diacetone acrylamide
DEGMA	Di(ethylene glycol) methyl ether methacrylate
DLS	Dynamic light scattering
DMA	N,N-dimethyl acrylamide
DMAEMA	N,N-dimethylaminoethyl methacrylate
DMF	Dimethylformamide
DMSO	Dimethyl sulfoxide
DNA	Deoxyribonucleic acid
DP	Degree of polymerization
DSC	Differential scanning calorimetry
EBS^-	p-Ethylbenzenesulfonate
FESEM	Field emission scanning electron microscope
HCOONa	Sodium formate
HPMA	2-Hydroxypropyl Methacrylate
KSPMA	Potassium 3-sulfopropyl methacrylate
LCST	Lower critical solution temperature
LiOTf	Trifluoromethanesulfonic acid lithium salt
MAPTAC	[3-(Methacryloylamino)propyl]trimethylammonium chloride
MEA	2-Methoxyethyl acrylate
M_n	Number average molecular weight
MOTAC	(2-(Methacryloyloxy)ethyl)trimethylammonium chloride
NMP	Nitroxide mediated polymerization
NMR	Nuclear magnetic resonance
NOESY	Nuclear Overhauser Effect spectroscopy
NTf_2^-	Bis(trifluoromethylsulfonyl)amide
OTf^-	Trifluormethanesulfonate
p	Packing parameter
P(OEtOxA)	Poly[oligo(2-ethyl-2-oxazoline)acrylate]
PAAC	Poly(allylammonium chloride)
PATAC	Poly(2-(acryloyloxy)ethyltrimethylammonium chloride)

PDAAM	Poly(diacetone acrylamide)
PDI	Polydispersity index
PDMAEMA	Poly(N,N-dimethylaminoethyl methacrylate)
PDPA	Poly(2-(diisopropylamino)ethyl methacrylate)
PEG	Poly(ethylene glycol)
PF_6^-	Hexafluoro phosphate
PGMA	Poly(glycerol monomethacrylate)
PHEMA	Poly(2-hydroxyethyl methacrylate)
PISA	Polymerization induced self-assembly
PMAA	Poly(methacrylic acid)
$PMEO_2MA$	Poly(di(ethylene glycol) methyl ether methacrylate)
PMOTAC	Poly(methacryl oxyethyl trimethylammonium chloride)
PMOTAI	Poly(methacryl oxyethyl trimethylammonium iodide)
PMPC	Poly(2-(methacryloyloxy)ethylphosphorylcholine)
PMVBIC	Poly(3-methyl-1-(4-vinylbenzyl)imidazolium chloride)
PNAGA	Poly(N-acroyloyl glycinamide)
PNIPAM	Poly(N-isopropylacrylaimde)
PVBTMAC	Poly((vinylbenzyl)trimethylammonium chloride)
PVBTPC	Poly(triphenyl-4-vinylbenzylphosphonium chloride)
RAFT	Reversible addition–fragmentation chain transfer polymerization
R_g	Radius of gyration
R_h	Hydrodynamic radius
ROMP	Ring opening metathesis polymerization
RT	Room Temperature
SbF_6^-	Hexafluoro antimonate
SCN^-	Thiocyanate
SEC	Size exclusion chromatography
T_{cL}	Clearing temperature
T_{cU}	Clouding temperature
TEM	Transmission electron microscopy
T_g	Glass transition temperature
UCST	Upper critical solution temperature
UV	Ultraviolet
VBTMA	(Vinylbenzyl)trimethylammonium

1 Introduction

1.1 Properties of polyelectrolyte solutions

Polyelectrolytes are ionic or ionizable macromolecules, which can dissociate into charged macromolecules and counterions in water or polar solvents.[1–3] Depending on the type of charge present in the polymer backbone or in the pendent group, they can be classified into polycations, polyanions, and polyzwitterions or polyampholytes. Polyampholytes contain both cationic and anionic groups either on the main chain or in the side chain,[4] whereas, in polyzwitterions, both positive and negative charges are present commonly on the same pendent group.[5] DNA, proteins and charged polysaccharides are examples of natural polyelectrolytes. Usually polyelectrolytes are highly soluble in water, and they have been used in many applications such as glues, flocculants in water treatment, emulsifiers, and additives in food and cosmetics, super absorbents, drug delivery, and in many others.[6–9]

Depending on the charge density and the degree of ionization, polyelectrolytes can be differentiated into strong or weak ones. However, their definition can vary depending on the point of view.[1] The strong polyelectrolytes are permanently charged ones, the solubility of which is not effected by pH. Examples for this group are polymers consisting of quaternary ammonium, phosphonium or sodium sulfate ionic groups. Polycarboxylic acids and polyamines are considered as weak polyelectrolytes. The solubility and the degree of ionization of these polymers varies with the pH.

Unlike nonionic polymers in organic media, solution properties of the polyelectrolytes are complex due to multiple types of interactions including long-range electrostatic interactions. Molar mass, ionic strength and polyion concentration have a strong influence on solution properties of the charged macromolecules. Considerable efforts have been made over the decades in understanding the polyelectrolyte solutions in terms of chain conformations and counter ion binding. Weak polyelectrolytes change their shape and size upon increasing the degree of ionization. This was observed by Katchalsky and Eisenberg for aqueous poly(methacrylic acid) (PMAA) solutions: when the solution pH increases above its critical value, the viscosity of a PMAA solution abruptly increases owing to the chain ionization followed by dramatic swelling of the chain.[10]

Strong polyelectrolyte chains possess long flexible or rigid rod conformations in dilute aqueous solutions. This is due to the electrostatic repulsions between repeating units of the same charge. In dilute solutions, the translational entropy of counterions is high and most of the counterions are released to the solution from the polyions. At finite polymer concentration, some of the counterions may condense on the polymer chain due to the strong electrostatic attraction between the charged units and counter ions.[11,12] With either increasing the polymer concentration or by decreasing the solvent quality, the number of condensed counter ions increases as the translational entropy of counterions decreases. Therefore, the effective charge on polyelectrolyte chains decreases, which further leads to polyelectrolyte chain shrinkage.[1,11–13]

Solubility of strong polyelectrolytes may change by screening the electrostatic interactions between charged repeating units with low molar mass salts. In high salt concentrations, polyelectrolytes act as nonionic polymers as the electrostatic interactions are exponentially screened, this leads to the domination of the short-range interactions. The solution properties

also depend on the valency of the counterions and interaction of solvent with ionic species. In low dielectric constant media, the polyelectrolytes form intra- and inter molecular ion pairs, which may lead to phase separation due to the dipolar interactions between the ionomer units.[13–17]

1.2 Phase separation of polycations in water

The water solubility of polyelectrolytes has been extensively studied in the presence of salts or other additives.[2,18] The solubility of weak polycations like poly(N,N-dimethylaminoethyl methacrylate) (PDMAEMA) and poly(2-(diisopropylamino)ethyl methacrylate) (PDPA) strongly depends on the pH and ionization degree of the repeating units. Their phase behavior is also dependent on the added salt at low pH ranges.[19–22]

Solubility of strong polycations is not affected by pH. However, their phase separation can be induced by certain salts. Few studies on the polycation brushes report on conformational transitions of polymers in aqueous solution induced by the ions from Hofmeister series (SO_4^{2-} > HPO_4^{2-} > CH_3COO^- > Cl^- > Br^- > NO_3^- > I^- > SCN^-). At high salt concentrations, cationic poly(methacryl oxyethyl trimethylammonium chloride) (PMOTAC) and poly((vinylbenzyl)trimethylammonium chloride) (PVBTMAC) brushes undergo a conformational transformation from fully stretched to collapsed coils due to the osmotic pressure changes within the brushes. The behavior is different in low salt regimes, polycation brushes collapse strongly with chaotropic ions than the kosmotropic anions. Because the cationic units form strong ion pair with chaotropic ions compared to the kosmotropic ones.[23,24]

Strong polycations with hydrophobic counterions may be insoluble in water. For example, aqueous solutions of cationic poly(allylammonium chloride) (PAAC) phase separate when introducing hydrophobic counterions like p-ethylbenzenesulfonate (EBS^-) ions.[25] The phase separation process of this polycation was studied by nuclear magnetic resonance spectroscopy (NMR), and results suggest the hydration changes around the cationic repeating units were mainly due to the hydrophobic EBS^- ions that replace the original Cl^- ions. This process can be reversed by screening the ionic interactions between the polyions and EBS^- with an excess of Cl^- ions. This phenomenon was also investigated for the solutions of styrene based PVBTMA with fluorescent hydrophobic ions. Excimer emission of pyrene sulfonate ions was observed in the presence of PVBTMAC, which confirmed the formation of hydrophobic domains.[26]

Solution properties of polycations differ significantly if instead of simple ions (Cl^-, Br^-, I^-, etc.), hydrocarbon counter ions are present in solution. The difference is especially noticeable for fluorinated counterions, such as tetrafluoroborate (BF_4^-), hexafluorophosphate (PF_6^-), trifluoromethanesulfonate (OTf^-), bis(trifluoromethylsulfonyl)amide (NTf_2^-). Polycations with fluorinated counterions may be insoluble in water but soluble in organic solvents.[27] Recently, it has been shown that water soluble cationic block copolymers may undergo a self-assembling process upon changing the counterions from Br^- to hydrophobic NTf_2^- ions.[28–30]

The solvent quality is one of the key parameters in counterion condensation. Changing the solvent, for example from aqueous to organic solvents, the free energy of the system is determined by Coulombic interactions. Consequently, in the solvents with low dielectric constant, strong ion pairing leads to intra- and inter molecular association. This has been demonstrated for a strong polycation, PMOTAC with methanesulfonate counterion. The

polycations undergo a reversible coil-to-globule transition upon increasing the acetone content in water-acetone mixtures.[31,32]

1.3 Thermoresponsive polymers

Water-soluble polymers phase separate when changing the thermodynamic quality of the solvent. The polymers that phase separate with changing temperature are called thermally responsive polymers. Polymers that phase separate upon heating are called with a lower critical solution temperature (LCST), whereas polymers phase separating upon cooling show an upper critical solution temperature (UCST) as shown in Figure ***1***. Poly(N-isopropylacrylamide) (PNIPAM) is a well-studied example of the LCST polymers.[33] PNIPAM is water-soluble at room temperature (RT) and phase separates above 32 °C. As water cages surrounding the PNIPAM units are disrupted with heating, the polymer chains start to aggregate. Poly(N-acryloyl glycinamide) (PNAGA) another nonionic aqueous polymer that shows the opposite phase behavior; due to the intra and inter molecular hydrogen bonding the polymer phase separates from water below UCST.[34]

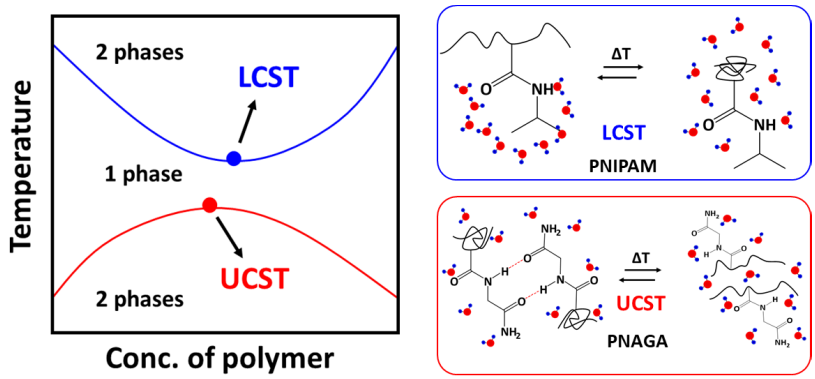

Figure 1 *Phase diagram of thermoresponsive polymers, LCST in NIPAM and UCST in PNAGA.*

Polyzwitterions also undergo an UCST-type phase transition in water due to the intra and inter molecular ionic interactions.[35–38] Several thermoresponsive polyanions in aqueous or non-aqueous systems have been reported in the literature.[39] For instance, anionic poly(styrene sulfonate) with tetrabutylphosphonium counterions show a LCST-type phase transition in aqueous solution. The LCST type behavior is mainly due to the hydration changes around the polyions units. Upon heating, polymers form random aggregates that are surrounded by cationic counterions. Similar phase transitions were also observed for methacrylate-based polyanions with tributylhexylphosphonium 3-sulfopropylmethacrylate ionic groups.[39–41]

1.4 LCST or UCST type phase transition in polycations

Cationic poly(tributyl-4-vinylbenzylphosphonium) bearing alkyl sulfonate ion pair was the first example reported to show a LCST-type phase transition in aqueous solutions.[42] An

LCST-type phase transition was also observed for similar polycation systems with either tributyl ammonium or tripentyl phosphonium cationic groups paired with alkyl sulfonate or chloride ions.[43,44] The cloud point temperatures of these entities are strongly dependent on the salt and polymer concentration.

Strong polycations with UCST-type phase transitions are vastly reported in the literature in comparison to those with LCST. Imidazolium-based polycations with tetrafluoroborate (BF_4^-) anions were the first reported to exhibit a UCST type transition in aqueous solutions. These polycations may also undergo LCST-type transitions in organic solvents if their counterions are exchanged from chlorides to SbF_6^-.[45] Poly(triphenyl-4-vinylbenzylphosphonium chloride) (PVBTPC) phase separates from its aqueous solutions with simple ions like Cl^-, Br^- and I^-.[46] In addition, this polycation can undergo an UCST-type phase transition with the cloud point temperature dependent on the polymer molar mass and the size of counterions.

Some polypeptides bearing various pyridinium and imidazolium cationic sidechains show UCST behavior in presence of BF_4^- counterions. When these polypeptides contain either oligo(ethylene glycol) as side chains or incorporated diethylene glycol linkages, they display LCST or both LCST and UCST phase transitions in presence of I^- or BF_4^-. The clouding behavior of the polymers is significantly dependent on the polymer and salt concentrations[47–50]

A weak polycation PDMAEMA, besides its pH responsiveness, can also show LCST in aqueous solutions. When NTf_2^- ions are present, PDMAEMA undergoes an UCST type phase transition; the behavior is strongly dependent on pH. Both the UCST and LCST behaviors may be observed by adjusting pH of PDMAEMA solutions when using multivalent counterions as cobaltate, chromate or hexacyanoferrate.[20,21,51]

The strongly charged poly[2-(methacryloyloxy)ethyltrimethylammonium] with different alkyl substitutions and BF_4^- as a counterion displays a UCST type transition.[52] However, the same polymer with iodide as a counterion (PMOTAI) is water-soluble at any temperature. Addition of hydrophobic counterion NTf_2^- to an aqueous solution of PMOTA leads to complete phase separation due to the strong binding of ions.[53] In the presence of NaCl or changing the counterions to trifluoromethanesulfonate (OTf^-) ions, a UCST-type phase transition can be induced. Similarly, the styrene based polycation, poly[3-methyl-1-(4-vinylbenzyl)imidazolium chloride] (PMVBIC) undergoes a UCST-type transition, though the reported cloud point temperatures are higher when compared to the PMOTAI under the same conditions. Less amount of triflate counterions is needed to make PMVBIC thermoresponsive due to the hydrophobic phenyl units. For both polymers, a sufficient ionic strength is required to observe the cloud/clearing point when using the NTf_2^- counterions. The cloud points can be tuned in a wide temperature window by changing the ionic strength of solutions.[53] Recently, a library of poly[trialkyl(4-vinylbenzyl)ammoniums] with different alkyl substituents on the ammonium units were investigated in several salt solutions. The polycation with ethyl substituents shows an UCST-type phase transition in presence of the OTf^-, SCN^-, and NTf_2^- counterions. With increasing the length of the alkyl substituents, the polycations undergo LCST-type transition in various salt solutions. The switch of the phase separation behavior from UCST to LCST was mainly attributed to changes in the hydration of the long alkyl chains surrounding charges.[54]

1.5 Thermoresponsive cationic copolymers

Several copolymers comprised of nonionic and cationic repeating units has been reported to show UCST or LCST phase transitions in aqueous solutions. The copolymers of poly(2-hydroxyethyl methacrylate) (PHEMA), with either weak cationic N,N-dimethylaminoethyl methacrylate (DMAEMA) or strong cationic [2-(methacryloyloxy)ethyl]trimethylammonium chloride (MOETAC), or [3-(methacryloylamino)propyl]trimethylammonium chloride (MAPTAC) undergo LCST and UCST phase transitions in aqueous solutions. PHEMA with low molecular weight shows an LCST-type phase transition. When copolymerized with charged units the thermoresponsive behavior of the copolymers changes from a single to a double thermally responsive one with both LCST and UCST. The double responsiveness of these polymers is mostly dependent on the NaCl concentration and also varies with the polymer concentration, polymer composition, or pH.[55]

The random copolymer P(OEGMA-co-BVIm[X]) comprising of oligo(ethylene glycol) methacrylate and imidazolium based cationic units shows a LCST phase separation in presence of SCN^-, BF_4^-, PF_6^- and NTf_2^- counterions.[56] Cationic copolymers of poly[oligo(2-ethyl-2-oxazoline)acrylate] P(OEtOxA) also exhibit LCST and UCST phase transitions in aqueous solutions. The thermoresponsive behavior can easily be tuned by adjusting the copolymer composition, the ionic strength and pH.[57]

The random copolymers of NIPAM and MPTMAC exhibit both LCST and UCST phase transitions in presence of NTf_2^- ions. These double phase transitions mainly occur when the copolymers consist of equal amount of NIPAM and AMPTAMC units. The copolymers undergo an LCST-type separation with the lower amount of AMPTMAC. Only the UCST-type separation has been observed for copolymers with high AMPTMAC content.[58]

Few cationic block copolymers are also known for thermoresponsive behavior, most of them reporting a LCST phase separation in water.[59–62] Above the critical temperature, one of the blocks phase separates while the other block remains soluble. Therefore, polymers can self-assemble into core-shell structures that consist of a stimuli responsive hydrophobic core coated with a hydrophilic outer shell. Block copolymers showing both the LCST and UCST behavior are of special interest. With changing temperature, the copolymers undergo disorder-order transitions or even build up inverse micelles. Thus, thermoresponsive copolymers can be used to encapsulate and release in a controlled way of poorly water-soluble active substances. The block copolymers comprised of weak polycation PDMEAMA and PEG or poly(di(ethylene glycol) methyl ether methacrylate) ($PMEO_2MA$) blocks undergo both UCST and LCST transitions are reported in the literature.[63,64] Depending on the pH and salt, poly(DMAEMA-b-MEO_2MA) diblock copolymer shows both UCST and LCST behavior. However, the behavior is mostly depend on the blocks composition, with high content of DMAEMA the thermoresponsive behavior may diseppear.[64]

1.6 Self-assembling of diblock copolymers

Upon phase separation, amphiphilic block copolymers build up various nano-objects such as spherical micelles, worm-like structures, and lamellae or vesicles upon varying the mole

fractions of the hydrophilic and hydrophobic units in the chain and/or the polymer concentration.[65,66] The morphology of the aggregates can primarily be determined by the packing parameter, $p = v/a_o l_c$, where a_o is the surface area of the hydrophilic block, v and l_c are the volume and the length of the hydrophobic block.[67–70] Altering these parameters, the copolymers can adapt various morphologies by adjusting the interfacial curvature (see Figure 2). If $p \leq ⅓$, spheres are formed; cylinders are formed when $⅓ < p \leq ½$; $½ < p \leq 1$ is for flexible lamellae or vesicles; and $p = 1$ is for planar lamellae. This applies for most of the surfactant molecules, which are at equilibrium. However, this may not be true for all the polymers as several other parameters like temperature, pH, and ionic strength, and solvent composition can also influence the morphologies of the copolymer aggregates.[65,71]

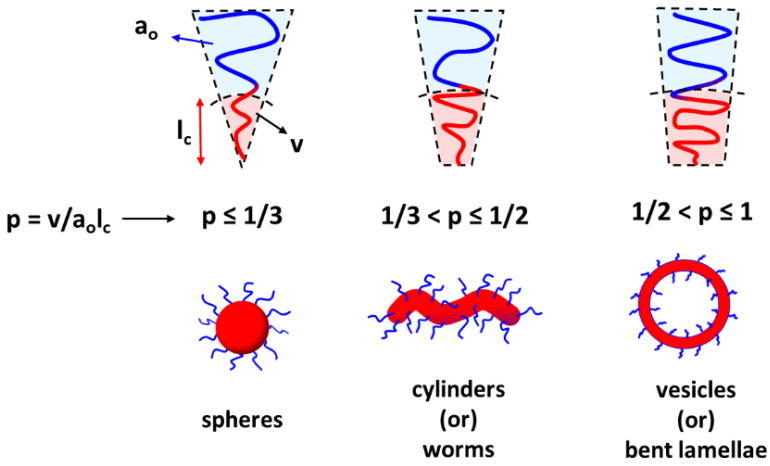

Figure 2 *The morphologies of diblock copolymer aggregates with different packing parameter.*

In the case of charged block copolymers, self-assembling behavior is similar to that of the ionic surfactants. The charge density and DP of the polyelectrolyte blocks influence the particle morphologies. The charge repulsions between the ionic groups can be tuned by changing the pH or salt concentration, and this may induce morphological changes.[72–76]

Typically, particles/aggregates consisting of diblock copolymers can be prepared by solvent exchange, or by thin film rehydration.[67,75] In the solvent exchange, the copolymers are first dissolved in a good solvent common for both blocks. Then, a selective solvent, which is a poor solvent for one of the blocks, is gradually added to the solution to induce the aggregation of polymers. Other recent approaches are microfluidic techniques[77] and in situ self-assembly of particles during the polymerization.[78,79]

1.7 Polymerization induced self-assembly

Polymerization induced self-assembly (PISA) has been widely used to synthesize amphiphilic nanoobjects with various morphologies including spheres, worms, vesicles, lamellae, toroids and other higher order morphologies.[80–84] The main advantage of PISA is that the particles can be synthesized at high solid concentration up to 50%, whereas the conventional methods are limited to only dilute conditions.[85] PISA can be conducted in either emulsion or dispersion polymerizations,[86] preferably with controlled radical polymerization (CRP) techniques such as atom transfer radical polymerization (ATRP),[87] reversible addition–fragmentation chain

transfer polymerization (RAFT),[88] nitroxide-mediated polymerization (NMP),[89] and ring opening metathesis polymerization (ROMP).[90–92] In PISA, the copolymers self-assemble during the controlled polymerization in which solvophilic chains are extended with another monomer that forms an insoluble block as shown in the figure 3.

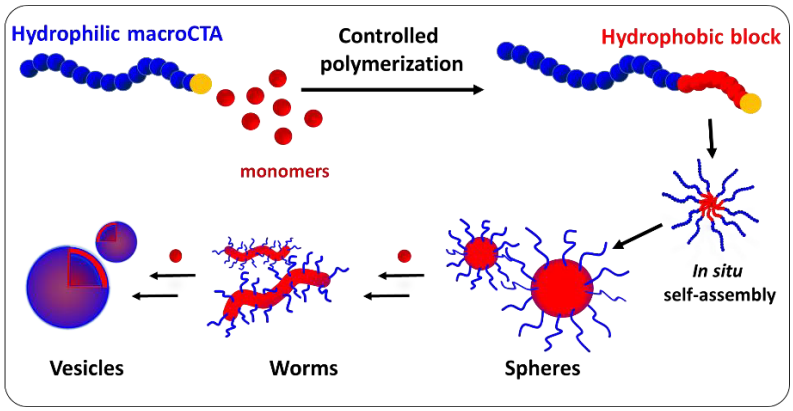

Figure 3 *Polymerization induced self-assembly of block copolymers via controlled radical polymerization.*

Compared to other techniques, well-defined nanostructures can be easily obtained by the RAFT dispersion polymerizations. Thus, most of the PISA systems reported are with aqueous RAFT dispersion polymerizations. PISA can be performed also in non-aqueous RAFT dispersion systems including polar and nonpolar solvents, supercritical CO_2, ionic liquids, or even in silicon and mineral oils.[93–100]

In PISA, higher order-morphologies are usually prepared by systematically increasing the DP of the core-forming block while keeping the stabilizer block length constant. In addition, increasing the copolymer concentration increases the probability of inelastic collisions between particles, thus effectively promoting morphological transitions.[101,102] Based on these two main parameters, a few morphological phase diagrams of copolymers exist in the literature. However, many other parameters such as initiator system, solvent composition, temperature, pH, stirring speed, and macroCTA end groups can also influence the particle morphology as in traditional methods. [103–108] The properties of core forming block such as the degree of solvophobicity and glass transition temperature (T_g) are also key parameters in PISA for synthesizing stable morphologies.[94,97,100,109]

A water-soluble monomer 2-hydroxypropyl methacrylate (HPMA) has been used as core forming monomer in many aqueous RAFT dispersion polymerizations.[110–112] Most of the vinyl monomers suitable for the core forming block suffer from the poor solubility in water.[78,94,113,114] However, a few water-soluble monomers include NIPAM, 2-methoxyethyl acrylate (MEA), di(ethylene glycol) methyl ether methacrylate (DEGMA), and diacetone acrylamide (DAAM) have been reported.[115–118]

Diacetone acrylamide is a water-soluble monomer while the polymer PDAAM is not, because of the hydrogen bonding interactions. Among the acrylamide-based monomers, DAAM has been recently utilized in several PISA syntheses.[119–121] Copolymer particles can be obtained when either ionic or nonionic stabilizing blocks are chain extended with DAAM. PDAAM as the single core block, particles with various morphologies including spheres, worms, lamella,

and uniform vesicles have been reported.[119] Recently, it has been demonstrated that when DAAM is copolymerized with N,N-dimethyl acrylamide (DMA) as core forming units, worms can be obtained with wide range of compositions.[120] Owing to the ketone functionalities, PDAAM core may be cross-linked via oxime or hydrazone modifications to tune the particle morphologies.[119,122–124] Higher-order morphologies have also be reported when linear or star PEG macroCTAs were chain extended with DAAM.[125]

1.8 Higher order morphologies with polyelectrolyte stabilizers

When polyelectrolytes are used as stabilizers, PISA polymerization often lead only to spherical structures, due to either steric repulsions between the long stabilizer blocks or charge repulsions among the corona chains.[66,85,112,126,127]

In early PISA works, RAFT aqueous emulsion polymerizations were extensively studied using polyanions and their copolymers as stabilizer blocks.[105,128,129] The latexes were prepared by chain extending poly(meth)acrylic acids with styrene or methacrylate-based hydrophobic monomers. Most of the copolymer latex particles were confirmed to have spherical structures. However, when using copolymers of (meth)-acrylic acid and ethylene oxide as stabilizers, the latexes with same hydrophobic blocks allowed the formation of particles with well-defined spheres, worms and/or vesicles in aqueous solutions.[130] The final morphologies of the particles were found to depend mainly on the molar masses of the hydrophilic and hydrophobic blocks. The other parameters, such as pH, salt, stirring speed and mole fractions of the acidic and nonionic ethylene oxide units in the stabilizer chains also effect the stability and morphology of the particles. Vesicular structures were observed, when poly(sodium acrylate) macrochains consisting of alkoxyamine end groups were extended with 4-vinylpyridine (4VP) via nitroxide mediated emulsion polymerization (at pH=11).[89]

When an anionic macroCTA, poly (potassium 3-sulfopropyl methacrylate) (KSPMA) was chain extended with 2-hydroxypropyl methacrylate (HPMA), aqueous RAFT dispersion polymerization only lead to loose hydrated aggregates.[112] This is due to the charge repulsions among PKSPMA stabilizer chains in the corona, which hinders the polymerization-induced self-assembly. However, diluting the strong anionic repulsions either by adding salt or statistically copolymerizing KSPMA with nonionic comonomers promotes spherical particles with dense cores. The latter approach enabled higher-order morphologies, when nonionic poly(glycerol monomethacrylate) (PGMA) macroCTAs were used as costabilzers to modulate the charges.

Polyzwitterions have also been used in PISA reactions for producing particles with fine-tuned morphologies.[110,111] A range of morphologies including spheres, worms and vesicles were accessed when phosphobetaine based poly(2-(methacryloyloxy)ethylphosphorylcholine) (PMPC) macroCTAs were chain extended with a hydrophobic core-forming monomer HPMA. Similar morphological structures were also obtained when sulfobetaine based macroCTAs were copolymerized with HPMA. In both cases the morphologies of particles were tuned either by changing the PHPMA block length or solids concentrations.

Few polycations have been used as macroCTAs in aqueous PISA to prepare charged nanoparticles.[131,132] In most cases, the particle morphologies were only spheres when the quaternary ammonium based polycation macroCTAs were used as sole stabilizer blocks.[126,133] However, morphological transitions can be triggered by reducing the charge repulsions in the corona analogous to discussed above. Worms and vesicles were produced from copolymers of HPMA using a mixture of nonionic macro chain transfer agent PGMA and cationic poly(2-(methacryloyloxy)ethyl trimethylammonium iodide) (PMOTAI).[134] Recently, a

similar quaternary ammonium based polycation, poly(2-(acryloyloxy)ethyltrimethylammonium chloride), PATAC, was chain extended with a core-forming monomer diacetone acrylamide (DAAM). The charge density in the corona was reduced using a binary mixture of PATAC and nonionic poly(N,N-dimethylacrylamide) as macroCTAs to obtain higher-order morphologies.[126]

A few PISA works have shown that addition of a cosolvent can also promote higher-order morphologies in ionic copolymer systems. However, the morphologies of the particles may also depend various parameters as stated above.[95,135]

1.9 Temperature, pH or salt induced morphological transitions

Serval aqueous PISA systems have shown that copolymers can undergo morphological transitions upon application of an external stimulus. Copolymer particles with poly(2-hydroxypropyl methacrylate) (PHPMA) hydrophobic cores have been reported to show thermally induced morphological transitions.[111,136–141] For example, free-standing gels obtained with poly(glycerol monomethacrylate)- poly(2-hydroxypropyl methacrylate) (PGMA-PHPMA) diblock copolymers undergo a reversible worm-to-sphere transition upon cooling to 4°C.[136,140,142] In addition, such PGMA-PHPMA diblock copolymers carrying acid end groups in the hydrophilic blocks exhibit both temperature and pH induced morphological transitions. The thermally induced transition was mainly attributed to the surface plasticization of PHPMA cores. pH-responsive behavior was driven by the ionization of carboxylic acid end-groups on PGMA stabilizer blocks.

However, the behavior is complex and dependent on the DP of core forming block. The vesicles obtained from copolymer HOOC-PGMA$_{43}$-PHPMA$_{250}$ only undergo morphological transition when exposed to both a pH and temperature switch. No morphological transitions were observed changing either of stimulus alone. With increasing the DP of PHPMA over 250, no morphology changes were observed with changing the solution pH. On the other hand, the copolymers with short DPs below 250 could undergo morphological transition from vesicles to either worms or spheres by switching the pH.[137]

The pH responsive morphological transitions also were observed for morpholine functionalized PGMA-PHPMA block copolymers.[143,144] At pH 3, the protonation of morpholine end-groups induces morphological changes either from vesicles to worms or worms to spheres. The process can be reversed with either by changing the pH or salt. The worms obtained with changing the pH can also further undergo thermal induced morphological changes from worms to spheres.[144]

Morphological transformations were observed also for the copolymers that comprising of zwitterion based poly(2-(methacryloyloxy)ethyl dimethyl-(3-sulfopropyl)ammonium hydroxide) PSBMA and PHPMA blocks.[111] A pure vesicle phase underwent sol-gel transition to form a mixture of worms and vesicles. De-gelation or worm to sphere transition was also observed when the block copolymer dispersion was cooled at 2 °C for 200 min.

Thermally induced morphological transitions from spheres to worms and vesicles or lamella have also been observed for the copolymers of PDAAM.[119,122] However, the transitions are rather weak to stimulus changes when comparing to the HPMA copolymer systems. Thermal behavior depends mainly on the composition of the core blocks. Block copolymer

$PDMA_{40}$-$PDAAM_{99}$ undergoes a morphological transition from worms to a mixture of vesicles and worms upon heating the dispersion to 50°C.[119] A weak pH responsive morphological change from pure worms to a mixture of worms and spheres was observed for the same block copolymers. The lamellae obtained from $PDMA_{30}$-$PDAAM_{70}$ copolymers at 70 °C were observed to transform to worms and spheres at 10 °C during 6 h.[122] This process was reversible, lamellae were reformed in 2 h when heated to back to 70 °C. In the cross-linked lamella, the morphological changes are however slow. Due to the crosslinking of the cores the morphological changes from lamella to worms/spheres were observed after 100h at 10 °C.

A few non-aqueous copolymers PISA systems have also been reported to undergo morphological transitions with changing stimulus conditions.[93,145,146] For instance, the diblock copolymer worms prepared by chain extension of poly[2-(dimethylamino)ethyl methacrylate]s with 3-phenylpropyl methacrylate via RAFT dispersion polymerization in ethanol underwent morphological changes from worms to spheres upon heating to 70 °C.[93] These temperature induced morphological transitions are rapid compared to the aqueous ones with PHPMA and PDAAM cores.

2 Objectives of the study

This study focuses on solution properties of polycations and cationic diblock copolymers and their self-assembling in aqueous solutions.

The first objective was to test the self-assembling of cationic diblock copolymers PEG-PVBTMA-OTf in the presence of triflate ions. The diblock copolymers were shown to be thermoresponsive. The interactions between the polymers and the counterions were investigated to understand the mechanisms of phase separation and particle formation. Effects of the lengths of the cationic blocks, as well as of the polymer end group were studied.

Secondly, the objective was to test the styrene-based polycations, PVBTMAC, as stabilizers in PISA. Dispersion polymerizations were conducted in aqueous sodium chloride solutions to tune the particle morphologies. In addition, it was shown the PVBTAMC-PDAAM particles may be turned to thermoresponsive with triflate ions.

The third objective was to compare three different polycations in PISA polymerizations. The main interest was to study the effect of the macroCTA on particle morphologies when changing the salt concentration and solids content. In addition, use of triflate ions in PISA was tested. The hydrophobic counterion can effectively screen the charges and it turns the cationic shells thermoresponsive. It was of interest to see, if morphological changes maybe induced by changing the temperature.

3 Experimental

Here, the experimental procedures and characterization methods are briefly summarized. The detailed procedures can be found in the respective publications I, II, III, IV, and in their supporting information.

3.1 Syntheses

3.1.1 Syntheses of homo and diblock copolymers of VBTMA-OTf [I, II]

The polymers were synthesized via controlled radical polymerization, RAFT, in aqueous solutions as shown in scheme 1. The monomer (vinylbenzyl)trimethylammonium trifluoromethanesulfonate (VBTMA-OTf) was first synthesized by counterion exchange from chloride to triflate in acetonitrile. The polymerizations were initiated with the azo-based initiator 4,4′-azobis(4-cyanovaleric acid) (ACVA) at 75 °C. Trithiocarbonate chain transfer agents, CPDTC (from Sigma) and poly(ethylene glycol) methyl ether 2- (dodecylthiocarbonothioylthio)-2-methyl- propionate (PEG macroCTA) with average M_n 5000 g mol^{-1} were used in the polymerizations of VBTMA-OTf. In the case of copolymers, the reagent ratios [monomer]:[CTA] were varied to obtain polymers with different molar masses. The monomer conversions and molar masses of the polymers were determined by ^{1}HNMR spectroscopy. One of the copolymers with short cationic blocks was reacted with AIBN to remove the aliphatic end group. The end group modification was confirmed by UV spectroscopy. The crude polymers were purified by dialysis.

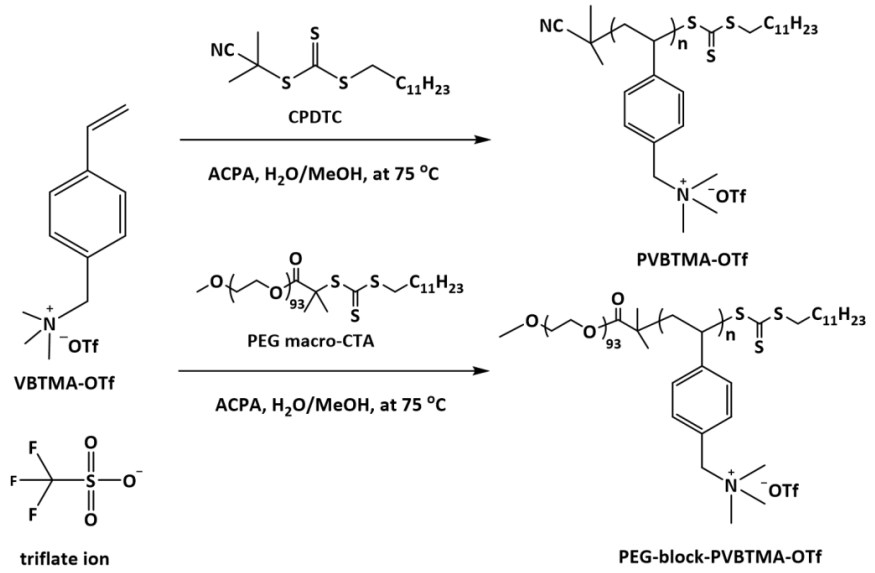

Scheme 1 *RAFT polymerization of VBTMA-OTf using CPDTC and PEG macroCTA.*

3.1.2 Syntheses of polycation macroCTAs [III, IV]

The polycation macroCTAs were synthesized via RAFT polymerization. In the case of PVBTMAC and PAMPTMAC the acid CTA, CTPA was used as shown in scheme 2. The polymerizations were conducted in aqueous solutions at 70 °C. For PMOTAC another chain transfer agent, CCTPA, was used. PVBTMACs with different molar masses were targeted by adjusting the molar ratio of monomer and CTA in the reactions. The monomer conversions were calculated from the ^{1}H NMR spectra. The macroCTAs were purified by dialysis.

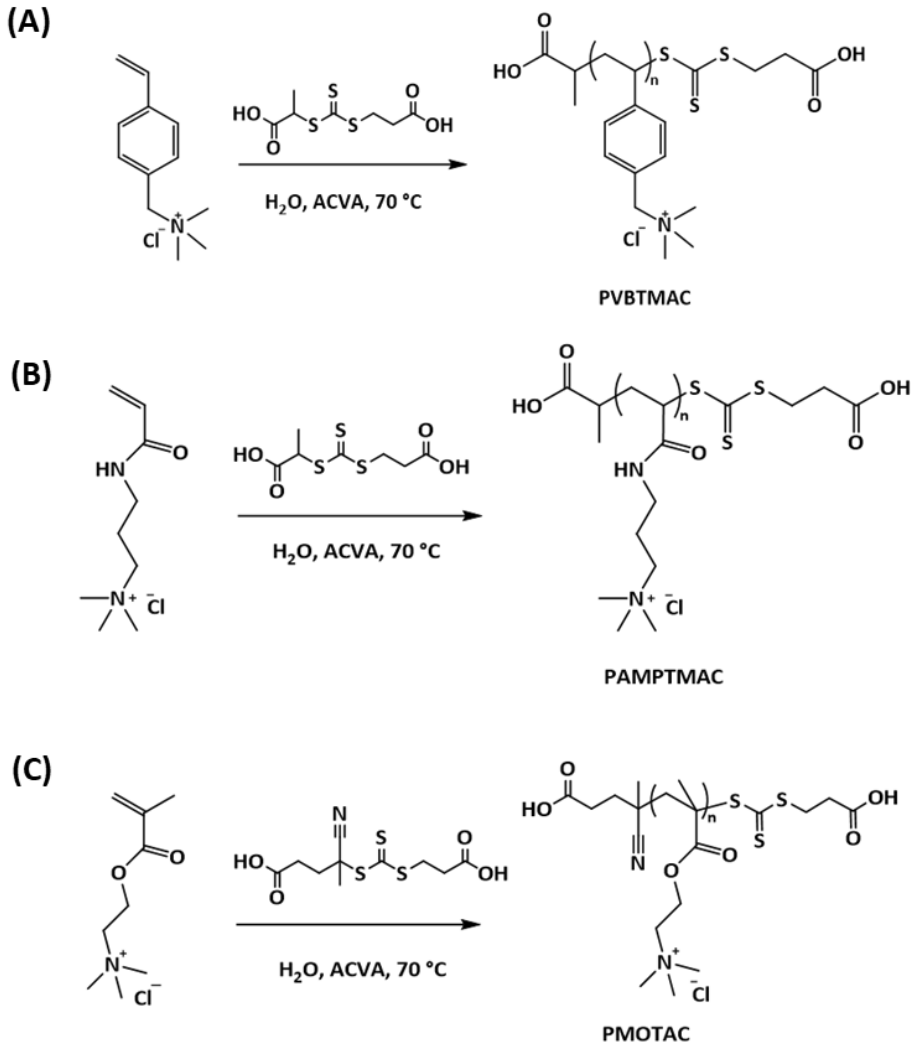

Scheme 2 *Syntheses of polycation macroCTAs via RAFT polymerization; A) PVBTMAC, B) PAMPTMAC and C) PMOTAC.*

3.1.3 Synthesis of polycation-PDAAM diblock copolymer particles[III, IV]

The polycation PVBTMAC macroCTA was chain extended with DAAM through RAFT aqueous dispersion polymerizations to synthesize copolymer particles. The reaction parameters, target DP of DAAM, NaCl concentration and solids content were changed. Next, PVBTMACs with three different molar masses and two more polycations, PAMPTMAC and PMOTAC were copolymerized in aqueous salt solutions changing parameters like [NaCl] or [LiOTf] and solids content. All polymerizations were initiated with ACVA at 70 °C. The polymerizations proceeded for 3h to reach the full monomer conversions. Detailed lists of the syntheses can be found in articles III, IV and their supplementary information.

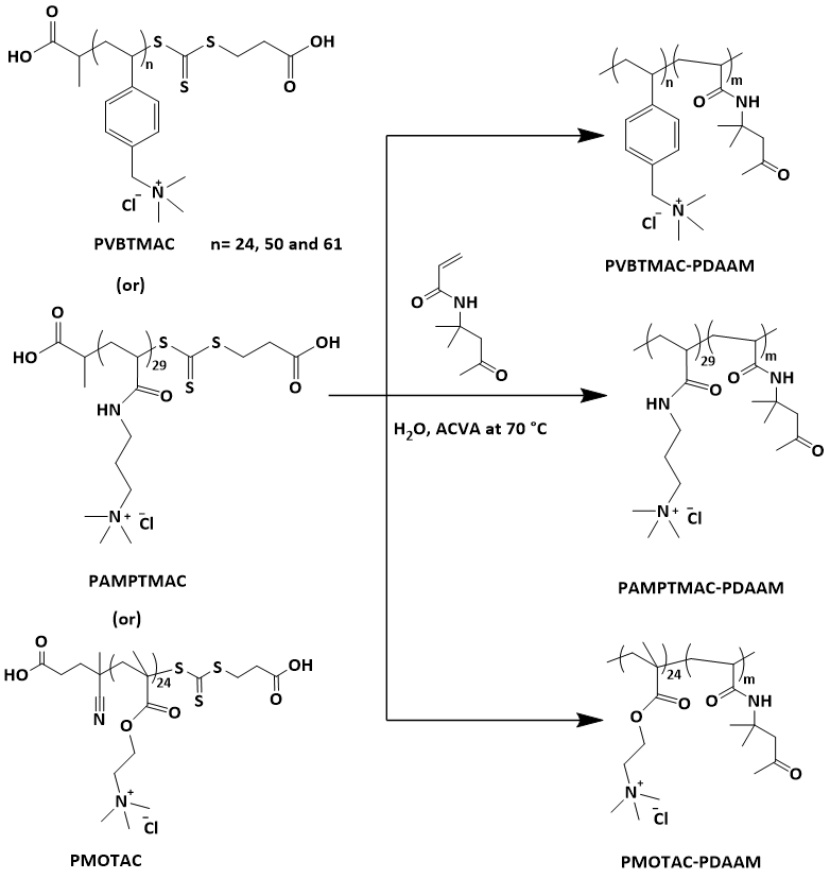

Scheme 3 *RAFT polymerization of DAAM using various cationic macroCTAs.*

3.2 Characterization methods

The NMR spectra were collected with Bruker Avance III 500 or 400 MHz spectrometers. The conversions of cationic monomers and DAAM were assessed in D_2O and DMSO-d_6. The spectra of all purified polycations and copolymers were recorded in D_2O, DMSO-d_6, or

methanol-d_4 at 25°C. Temperature variant ^{1}H NMR spectra were measured in D_2O solutions using sodium formate (HCOONa) as reference.[I, II] The polymer concentration was 2 mg mL^{-1} in 50 mM aqueous LiOTf. The two-dimensional nuclear Overhauser effect spectroscopy (NOESY) experiments were conducted with mixing time of 256 ms.

The molar mass distributions of the polymers were obtained by size exclusion chromatography (SEC). The set up equipped with Waters 515 HPLC pump, Biotech DEGASi GPC degasser, Waters 2410 differential refractometer, Waters 2487 Dual λ absorbance detector and column set Ultrahyhdrogel 120, 250 and 2000 was used to collect the eluograms. For polycation macroCTAs water/acetonitrile (60/40) with 0.1% trifluoroacetic acid was used as an eluent and poly(ethylene oxide) standards were used for the calibration.

JASCO V-750 UV–vis spectrophotometer equipped with a JASCO CTU-100 Peltier thermostat system was used for end group analysis. The same spectrophotometer or JASCO J-815 CD spectrometer equipped with a PTC-423S/15 Peltier temperature control system was used for most of the transmittance measurements. The transmittance of the solutions was measured as a function of temperature at 600 nm wavelength. Heating and cooling rates were 1 °C min^{-1} unless otherwise mentioned. The experiments were typically conducted by stabilizing samples for 10 min at starting temperatures.

Thermograms of the polymer solutions were obtained with a Malvern MicroCal PEAQ DSC microcalorimeter. The samples were stabilized for 10 min prior to the measurements. The cooling and heating rates were always 1 °C min^{-1} unless otherwise mentioned.

Temperature or angular dependent scattered light intensity of the copolymer solutions was measured using a Brookhaven instrument equipped with BI-200SM goniometer, BIC-TurboCorr digital pseudo-cross-correlator, and BI-CrossCorr detector. All measurements were conducted at 637 nm on aqueous solutions with 2 mg mL^{-1} of polymer and 50 mM of LiOTf. Temperature-dependent intensities and size distributions of the polymer solutions were measured using Malvern Instruments ZetaSizer Nano-ZS equipped with a 4 mW He–Ne laser operating at 633 nm. Measurements were performed in the temperature range 90–20 °C with back scattering at 173°. The samples were allowed to equilibrate for 3 min at each temperature. The hydrodynamic diameters, size distributions, zeta potentials and electrophoretic mobilities of the PISA particles were measured from the dispersions (0.1 w/w %) at 25 °C.

JEOL JEM-1400 transmission electron microscope (Jeol Ltd., Tokyo, Japan) fitted with an Orius SC1000B bottom mounted CCD-camera (Gatan Inc., USA) operating at 80-120 kV was used for TEM imaging of the particles. The samples were placed on glow discharged carbon coated Copper grids. The anionic stain, uranyl acetate (3 wt. %) was used for better contrast.

4 Results and discussion

In this section, first, the syntheses of homo and diblock copolymers, PEG-PVBTMA-OTf, and their solution properties will be discussed. Later discussions will be focused on the PISA polymerization of cationic diblock copolymers and thermoresponsive behavior of the particles.

4.1 Syntheses of polymers

4.1.1 PVBTM-OTf and PEG-VBTMA-OTf [I, II]

The styrene-based cationic monomer VBTMA-OTf was obtained by anion exchange from Cl^- to OTf^- and it was polymerized via RAFT using trithiocarbonate-based CTAs. The reaction mixtures of all the polymers were transparent at elevated temperature 75 °C. However, the phase separation of polymers was observed upon cooling to room temperature. This behavior indicated the UCST-type thermoresponsiveness of the polymers. The purified polymers were soluble in water and mainly characterized by NMR spectroscopy. The average degrees of polymerization (DP) and molar masses of the pure polymers were determined by ^{1}H NMR. The proton peaks ($–CH_2$) of PEG chains were taken as reference to determine the final ratio of the two blocks. The relative ratio of the proton signal ($–CH_3$) of the aliphatic end group to the aromatic proton signal from PVBTMA-OTf was taken to calculate the molar mass of the homopolymer. The details are summarized in table 1. Due to either poor solubility of the polymers or adsorption to the columns the SEC measurements conducted with water/$NaNO_3$ and in DMF/LiBr as eluents were not successful. The diblock copolymer VB_{62} (entry2 in table1) was reacted with AIBN to remove the aliphatic CTA end group. The disappearance of trithiocarbonate absorption from the UV-Vis spectra confirmed the dissociation of the end group. For simplicity, the diblock copolymers are denoted as VB_n based on their DP of the cationic blocks.

Table 1 *Homopolymer PVBTMA-OTf and diblock copolymers VB_n obtained via RAFT polymerization.* [I, II]

entry	polymer	[a]DP $_{NMR}$	[b]$M_{n\ Theo}$ (g/mol)	[a]$M_{n\ NMR}$ (g/mol)	[a]ratio $_{NMR}$ [PEG]:[PVBTMA]
1	PVBTMA-OTf	60	30000	20100	-
2	VB_{62}	62	30000	25000	1:0.67
3	VB_{81}	81	36500	30700	1:0.90
4	VB_{172}	172	67700	60900	1:1.90
5	VB_{270}	270	125900	92700	1:2.90

a. The molar mass and block ratios were determined by ^{1}H NMR.
b. Theoretical molecular mass from the equation [M] / [CTA] × conversion % × $M_{monomer}$ + M_{CTA}. M_n of the PEG macroCTA 5000 g/mol (from Sigma), M_n from SEC is 4900 g/mol with PDI 1.01, and the average DP from ^{1}H NMR is 93.

4.1.2 Cationic macroCTAs

Five styrene based PVBTMAC$_n$s with various DPs, as well as methacrylate based PMOTAC and acrylate based PAMPTMAC were synthesized via RAFT polymerization. The mean DPs and molar masses of the polymers determined with NMR and SEC are listed in table 2. In the case of PVBTMAC$_n$ and PAMPTMAC macroCTAs, methyl proton peaks (3H, -CH_3 around 1 ppm) from CTPA were used to determine the final DPs and molar masses of the polymers. The proton peak at 2.25 ppm from CCTPA was used to calculate the final DP and molar mass of the PMOTAC macroCTA. The SEC experiments conducted using water/acetonitrile as an eluent were successful and polydispersity indices are reported in table 2.

Table 2 *List of polycation macroCTAs synthesized via RAFT polymerization.* [III, IV]

entry	macroCTA	CTA	[a]$M_{n\ (theo)}$ (g/mol)	[b]$M_{n\ (NMR)}$ (g/mol)	[b]DP (NMR)	[c]$M_{n\ (SEC)}$ (g/mol)	[c]$PDI_{(SEC)}$
1	PVBTMAC$_{21}$	CTPA	5120	4725	21	-	-
2	PVBTMAC$_{27}$	CTPA	5430	5970	27	4730	1.20
3	PVBTMAC$_{24}$	CTPA	5700	5330	24	5100	1.27
4	PVBTMAC$_{50}$	CTPA	11300	10900	50	8750	1.30
5	PVBTMAC$_{61}$	CTPA	14100	13100	61	10550	1.36
6	PAMPTMAC$_{29}$	CTPA	5900	6300	29	6230	1.30
7	PMOTAC$_{24}$	CCTPA	6300	5300	24	5770	1.34

a. Theoretical molecular mass from the equation [M] / [CTA] × conversion % × $M_{monomer}$ + M_{CTA}.
b. The DPs and molar masses were determined by ^{1}H NMR.
c. The molar masses and PDIs are determined from SEC.

4.2 UCST-type phase transition of cationic homopolymers

All the homopolymers (entry 1 in table 1, and entries 2-7 in table 2) are well soluble in water at any temperature. The styrene-based polycations bearing either OTf^- or Cl^- phase separate in aqueous LiOTf solutions, the behavior is similar to that of UCST type polycations.[46,53] For the PVBTMA-OTf, a small amount (10 mM) of LiOTf induced phase separation when polymer concentration was 1 mg mL^{-1}. With increasing the salt concentration up to 100 mM, the polymer was completely precipitated. This indicates the competition between dissociation and strong ion pairing at the surface of the phase separated aggregates. In low salt concentrations the charged groups near the surface may dissociate, thus stable colloids were formed below the cloud point temperatures. However, when a significant amount of triflate ions is added in the solution, the charge dissociation becomes less favorable due to the strong ion pairing. Subsequently, binding of hydrophobic counterions to the surface of the formed aggregates leads to complete precipitation.

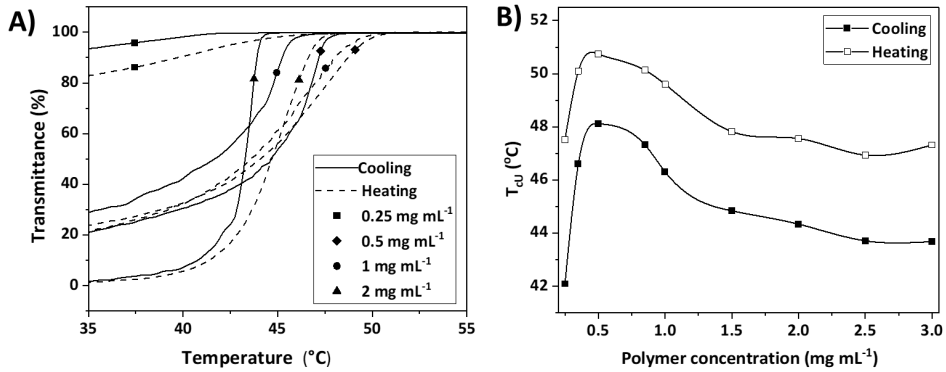

Figure 4 (*A) Transmittance curves for PVBTMA-OTf solutions with various polymer concentrations and constant LiOTf concentration (30 mM) and (B) the cloud point temperatures (T_{cU}) as a function of PVBTMA-OTf concentration.* [1]

The transmittance curves and cloud point temperatures collected for various PVBTMA-OTf concentrations are shown in figure 4. The cloud point T_{cU} reached a maximum at 0.5 mg mL^{-1} and decreased with further increasing the polymer concentration. Reversible phase transitions from insoluble to soluble were observed upon heating, with thermal hysteresis of ~5 °C. The phase separation and mixing processes observed with microcalorimetry were in line with the transmittance results and very sharp exothermic peaks were obtained upon cooling.

In the case of polycations bearing chloride ions, higher amount of LiOTf is needed to induce the phase separation. In the presence of 100 mM LiOTf, the styrene-based polycations with short DPs undergo phase separation below 40 °C. However, the behavior is strongly dependent on the molar mass of the polymers. With increasing the molar mass of PVBTMAC, the cloud point shifted to higher temperatures while keeping the LiOTf concentration constant (figure 5). Similar phase transitions were observed for the imidazolium based polycations with BF_4^- anions; the T_{cU} was mostly dependent on the polymer concentration but not on the molar mass of polycations.[45] The other two polycations PMOTAC and PAMPTMAC do not phase separate at any temperature when using the same polymer and LiOTf concentrations as in the case of PVBTMAC. The solution behavior of these polycations are in good agreement with previous studies on chemically different polycations.[53] Due to the aromatic functionalities, the styrene based polycations needed less hydrophobic counterions to induce the phase separation, whereas the PMOTAI phase separates with higher amount LiOTf.

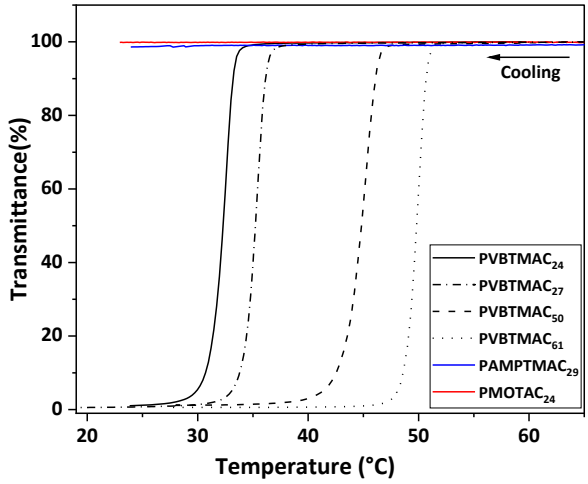

Figure 5 *Transmittance cooling curves for polycations (1 mg mL^{-1}) in 100 mM aqueous LiOTf solutions.*

4.3 Stepwise phase separation of block copolymer (VB_{81})[l]

The phase separation of the block copolymer VB_{81} was investigated by various methods in aqueous LiOTf solutions. The block copolymer was well soluble in pure water, but phase separated upon addition of LiOTf. UCST-type phase transition was induced in VB_{81} (1 mg mL^{-1}) by introducing 40 mM of LiOTf. A stepwise phase separation was observed for the aqueous VB_{81} solutions in a certain range of LiOTf concentrations (from 50 to 80 mM), see figure 6. The polymers first underwent UCST-type phase transition below the clouding temperature (T_{cU}), but the solutions became partially clear upon further cooling to room temperature. The behavior, however, was complex and dependent on the LiOTf concentration. As shown in figure 6, no clearing transition was observed for the polymer solutions with 100 mM or higher LiOTf concentrations. T_{cL} data could not be collected from the heating curves, as they do not follow the same trends as the cooling curves, and several steps were observed.

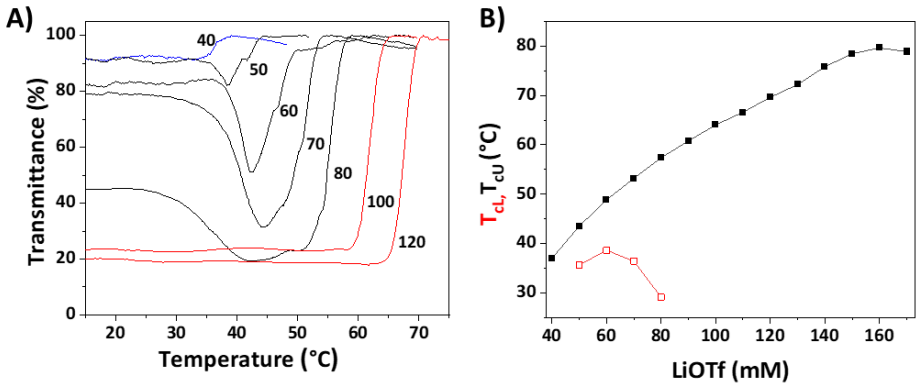

Figure 6 *Transmittance cooling curves for block copolymer VB_{81} (1 mg mL^{-1}) aqueous solutions with various LiOTf concentration (A) and corresponding clouding (T_{cU}) and clearing (T_{cL}) temperatures (B).* [1]

The transmittance cooling curves for the aqueous solutions with various polymer concentration are shown in figure 7. Interestingly, with constant LiOTf concentration (50 mM) VB_{81} undergo stepwise phase separation at any polymer concentration. Both clouding and clearing transitions were observed upon cooling. With increasing the polymer concentration, T_{cU} increases up to certain concentration (2 mg mL^{-1}). Cation-to-anion ratio was approximately 1:10 in the solutions with 2 mg mL^{-1} polymer concentration. No increase in T_{cU} was observed at high polymer concentrations because the cation-to-anion ratio decreased with increasing the polymer concertation at constant LiOTf.

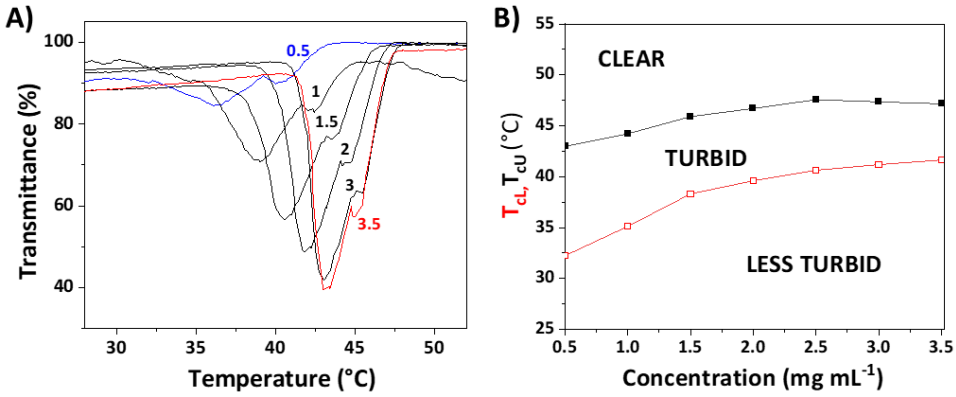

Figure 7 *Transmittance cooling curves for block copolymer VB_{81} aqueous LiOTf (50 mM) solutions with various polymers concentration (A) and corresponding clouding ($T_{cU,}$ ■) and clearing ($T_{cL,}$ □) temperatures (B).*[1]

The stepwise phase separation was studied further with Micro-DSC, DLS and NMR. Cooling thermograms obtained with different polymer concentrations show broad and stepwise transitions that coincided with the transmittance results. The enthalpy changes obtained from both cooling and heating thermograms associated with the phase separation process are shown in figure 8.

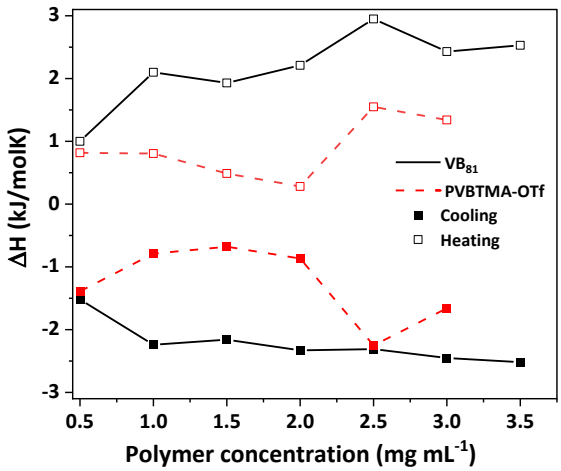

Figure 8 *The enthalpy changes obtained from both cooling and heating thermograms of VB_{81} and PVBTM-OTf solutions in the presence of LiOTf.*[1]

The phase separation process of VB_{81} (2 mg mL^{-1}) in 50 mM LiOTf solution was studied by DLS. The scattered light intensity and size distributions collected at different temperatures are shown in the figure 9 together with a photograph of the dispersions. At 55 °C or above, low scattering intensity indicates the dissolution of polymer. A small number of large aggregates may be present in solution. Light scattering intensity increases upon cooling below 42 °C due to worsening of the solvent quality, and polymers phase separate into aggregates with diameters over 1000 nm. At 25 °C, the diameter of these aggregates is of the order of 100 nm, and the R_g/R_h ratio is of the order of 1.0, obviously indicating the presence of particles with loose cores. The changes in the scattering intensity upon heating also confirms the reversible stepwise phase separation. First, the scattering intensity increased upon heating as the particles started to dissociate. Above 45 °C, a sudden decrease of intensity was observed as the polymers dissolved upon heating.

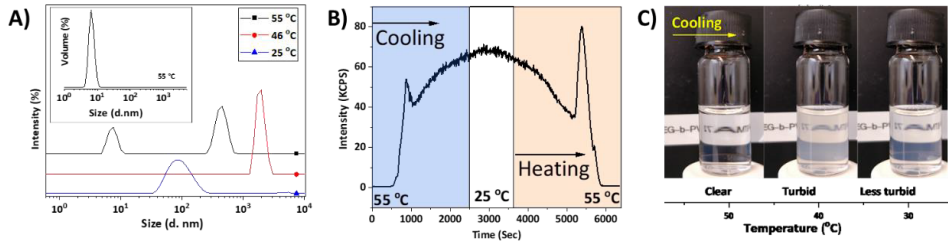

Figure 9 *DLS data collected for the aqueous VB_{81} (2mg mL^{-1}) solutions with 50 mM LiOTf. A) Size distributions obtained at various temperatures, B) Scattered light intensity upon cooling and heating cycle, and C) the photograph of solution at different temperatures.*[1]

The stepwise phase separation was only possible when PEG was covalently bound to the cationic block. This was confirmed by the transmittance cooling curves collected for mixed polymers solutions, as shown in the transmittance curves a-c in figure 10. The stepwise phase transition was affected by adding extra PEG macroCTA to the diblock copolymer solutions (a). Addition of cationic homopolymer to the diblock copolymer solutions led to a single phase transition (b). Importantly, only one sharp phase transition was observed for the mixture of

PEG macroCTA and polycation in triflate solutions, when nearly equal molar amounts of repeating ether and cation units as in VB_{81} were used (c).

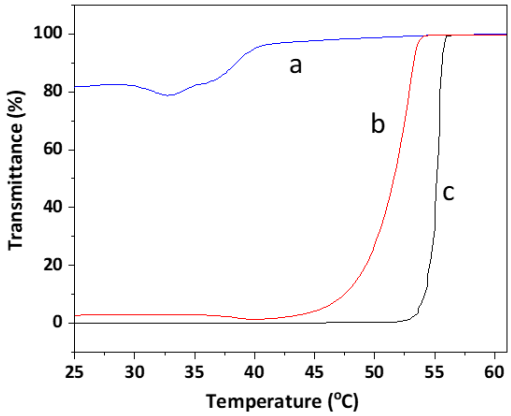

Figure 10 *Transmittance cooling curves of a mixed polymer solutions with 50 mM LiOTf. A mixed solution of PEG and VB_{81} (a), a mixed solution of PVBTMA-OTf and VB_{81} (b), and a mixed solution of PEG and PVBTMA-OTf (c).* [1]

4.4 Molar mass effect on phase separation [II]

The stepwise phase separation of the block copolymer PEG-PVBTMA-OTf was further investigated by changing the molar mass of the cationic block. Solution properties of the diblock copolymers VB_{62} with short, and two with long cationic blocks VB_{172} and VB_{270} were studied in aqueous LiOTf solutions.

4.4.1 Diblock copolymer with a short cationic block, VB_{62}

The copolymer VB_{62} undergoes a stepwise phase separation in the presence of triflate ions, similarly to VB_{81}. The transmittance cooling curves obtained for VB_{62} (1mg mL^{-1}) with different LiOTf concentrations (0 to 1M LiOTf) are shown in the figure 11A. Upon cooling, the clear polymer solutions turned cloudy below T_{cU} and then became clear at T_{cL} with further cooling. The behavior differs from VB_{81}, with increasing the salt concentration up to 400 mM LiOTf the insolubility window became wider and stepwise clearing was observed. The transmittance reached almost 100% above the clearing temperature, whereas in the case of the VB_{81} the clearing points disappeared with increasing the salt concentration. Above 400 mM LiOTf, the cloud points shifted to lower temperatures and insolubility windows became narrow with increasing the LiOTf concentration.

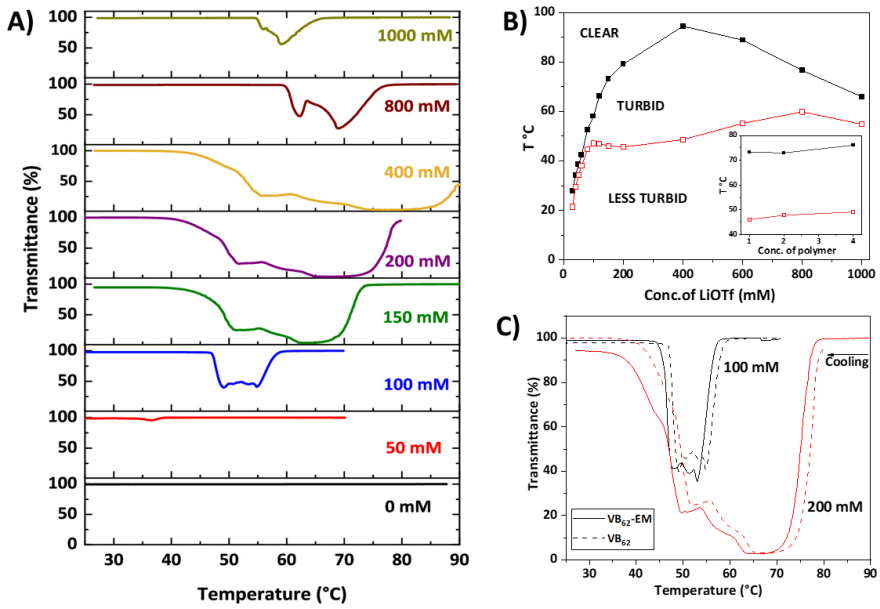

Figure 11 *Transmittance cooling curves of aqueous VB_{62} solutions with various LiOTf concentration (A). Clouding ($T_{cU,}$ ■) and clearing ($T_{cL,}$) temperatures with varying LiOTf; T_{cU} and T_{cL} with different polymer concentration are shown in inset (B). Transmittance cooling curves obtained for end group modified VB_{62} with 100 and 200 mM LiOTf concentration (C).* [II]

The polymer solution with 150 mM LiOTf, studied with different cooling rates showed only minimal changes in the phase separation process. However, the polymer phase separated in a stepwise manner at any cooling rate. In figure 11B, the clouding and clearing point collected from the cooling transmittance curves are plotted as a function of LiOTf concentration. A similar trend was also observed upon heating, the solution clouded stepwise at T_{cL} upon heating and cleared again at high temperatures (T_{cU}). The polymer concentration has no effect on the phase separation process, see inset figure 11B. The end group was removed from VB_{62}. The phase separation processes of VB_{62} and VB_{62}-EM (end group removed) were similar. Removing the hydrophobic end groups shifted the cloud points to slightly lower temperatures, however (figure 11C).

4.4.2 High molar mass polymers, VB_{172} and VB_{270}

The phase separation of the block copolymers with long cationic blocks VB_{172} and VB_{270} differed from the other two copolymers. In the presence of 20 mM of LiOTf, both copolymers (1mg ml^{-1}) showed the UCST-type phase transition around ambient temperature. With increasing the salt concentration, the cloud point shifted to higher temperatures (figure 12). However, the copolymers underwent only one sharp UCST-type phase transition. No clearing was observed for either polymer dispersions.

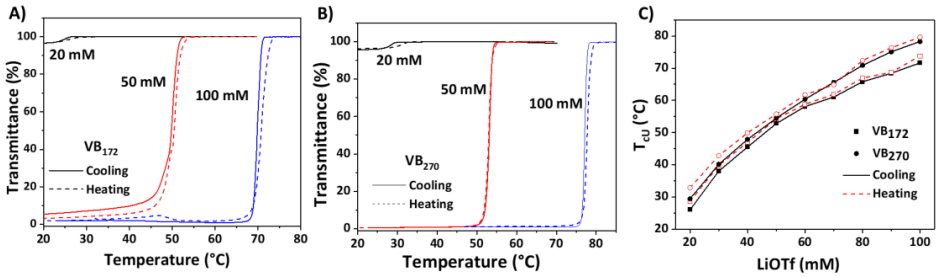

Figure 12 *Transmittance curves for (A) copolymer VB_{172}; (B) copolymer VB_{270} in LiOTf solutions with constant polymer concentration (1 mg mL^{-1}). C) Cloud point temperatures of both polymers as function of LiOTf concentration.* [II]

Overall, length of the polycation block turned out to have a critical effect on the thermal behavior of the polymers. The transmittance curves obtained for all block copolymers in aqueous 50 mM LiOTf are shown in figure 13. With short cationic blocks, the polymers undergo stepwise phase separation. First, the cationic blocks undergo an UCST-type phase transition below T_{cU}, and then stabilized by hydrophilic PEG blocks below the clearing temperatures T_{cL}. As the number of the cationic units increased, the phase separation of the polymers took place in one step. The behavior of the longest polymers resembled that of the homopolymers and indicated the formation of unstable aggregates.

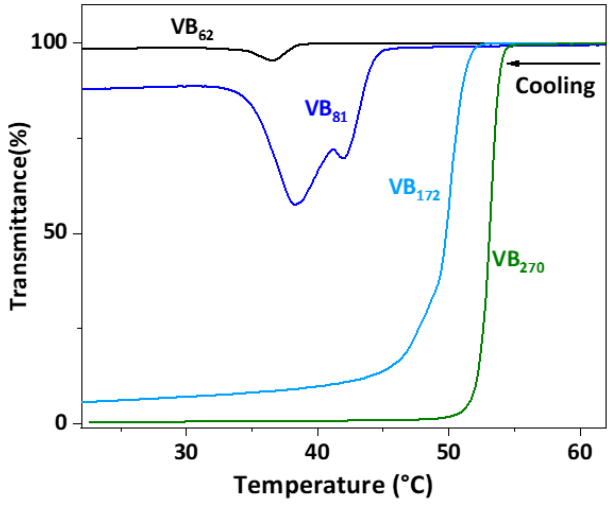

Figure 13 *Transmittance curves upon cooling, copolymers VB_{62}, VB_{81}, VB_{172}, and VB_{270} in 50 mM LiOTf solutions with constant polymer concentration (1 mg mL^{-1}).* [II]

The transmittance data were complemented by light scattering studies on the copolymer solutions. The size distributions measured at different temperatures for the copolymer solutions are shown in figure 14. At 75 °C, the copolymers showed bimodal size distributions with the smallest sizes below 10 nm, which indicated the polymers were dissolved on molecular level. Upon cooling VB-62 solution (2 mg mL^{-1}, 150 mm LiOTf), the polymer formed very large aggregates, of the order of 1000 nm at 55 °C. However, upon further cooling to 50 °C and below, the large aggregates gradually dispersed in to small ones, with diameters below 100 nm. The copolymers with long cationic blocks formed large aggregates at 50 °C, however, these did not disintegrate into small aggregates upon further cooling to 25 °C.

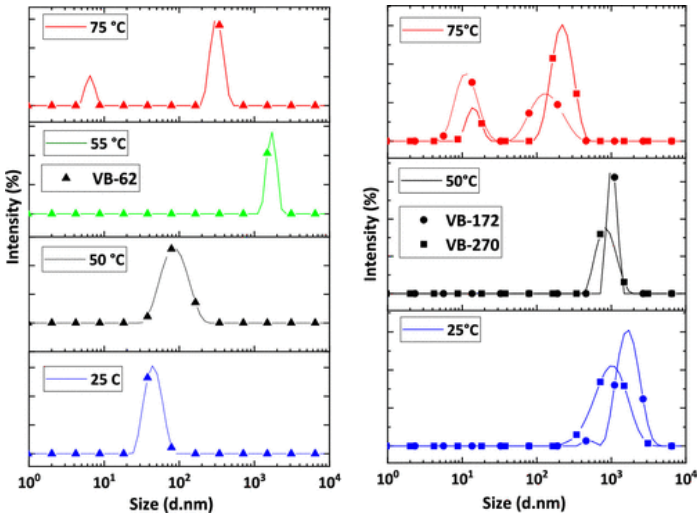

Figure 14 *Size distributions measured at 173° scattering angle for VB-62 (▲) in 150 mM (left) and VB-172 (●) and VB-270 (■) (right) in 50 mM LiOTf solutions, polymer concentration 2 mg* mL^{-1}.[II]

4.4.3 Phase separation observed by NMR

The phase separation of the block copolymers was also investigated by ^{1}H NMR measurements. The ^{1}H NMR spectra collected at various temperatures for the copolymer solutions (2 mg mL^{-1}) are shown in figure 15. At 75 °C the copolymers are well soluble, thus the proton peaks/signals from the both blocks are visible. However, in all cases (A-C), the signals of the cationic block disappeared upon cooling to 25 °C because of the phase separation. Only proton peaks from ethylene glycol units were observed at lower temperatures. The temperature dependent splitting of the PEG signal was observed in the presence of LiOTf or NaCl. The splitting of the PEG signal was different in copolymers and dependent on the salt concentration, and no splitting was observed in pure D_2O at any temperature. At 25 °C, broadening of the proton peaks of PEG units occurred with increasing the cationic block length. The broadening of the PEG signals indicated that most of the polyether was buried in the cores of the particles and only few free chains were dangling on the surface in the case of high molar mass polymers VB_{172} and VB_{270}. On the other hand, the sharp PEG signal in the case of VB_{61} indicated that PEG chains were in mobile state and acted as steric stabilizers for the phase separated cationic cores. In addition, splitting of the PEG signal indicated the counterion mediated interactions in the presence of salts.

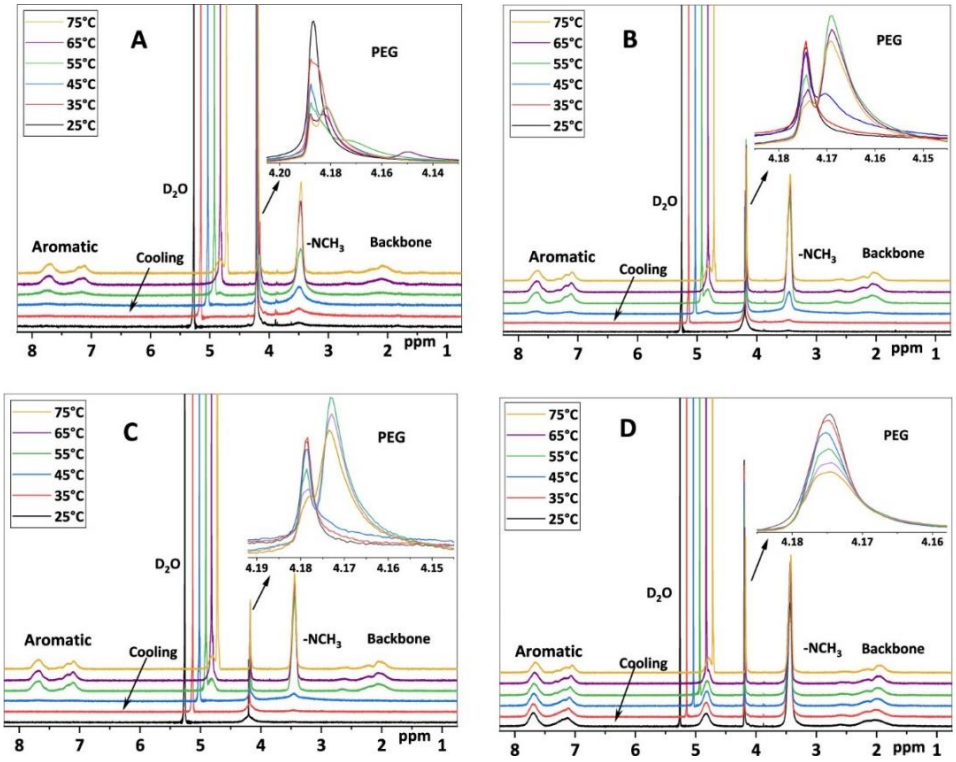

Figure 15 *[1]H NMR spectra of copolymers collected at various temperatures upon cooling: (A) 2 mg mL^{-1} of VB-62 in 150 mM LiOTf, (B) 2 mg mL^{-1} of VB-172 in 50 mM LiOTf, (C) 2 mg mL^{-1} of VB-270 in 50 mM LiOTf, and (D) 2 mg mL^{-1} of VB-172 in pure deuterated water.* [II]

The phase separation process of the copolymers was further studied with two-dimensional ^{1}H-^{1}H NOESY spectra measured at various temperatures. Weak cross-peaks between the PEG and −NCH_3 protons from cationic blocks were observed within the temperature range from 70 to 40 °C for VB_{62} in D_2O with 150 mM LiOTf. In the case of the high molar mass polymers, strong cross-peaks were observed below the cloud point suggesting interactions between two blocks.

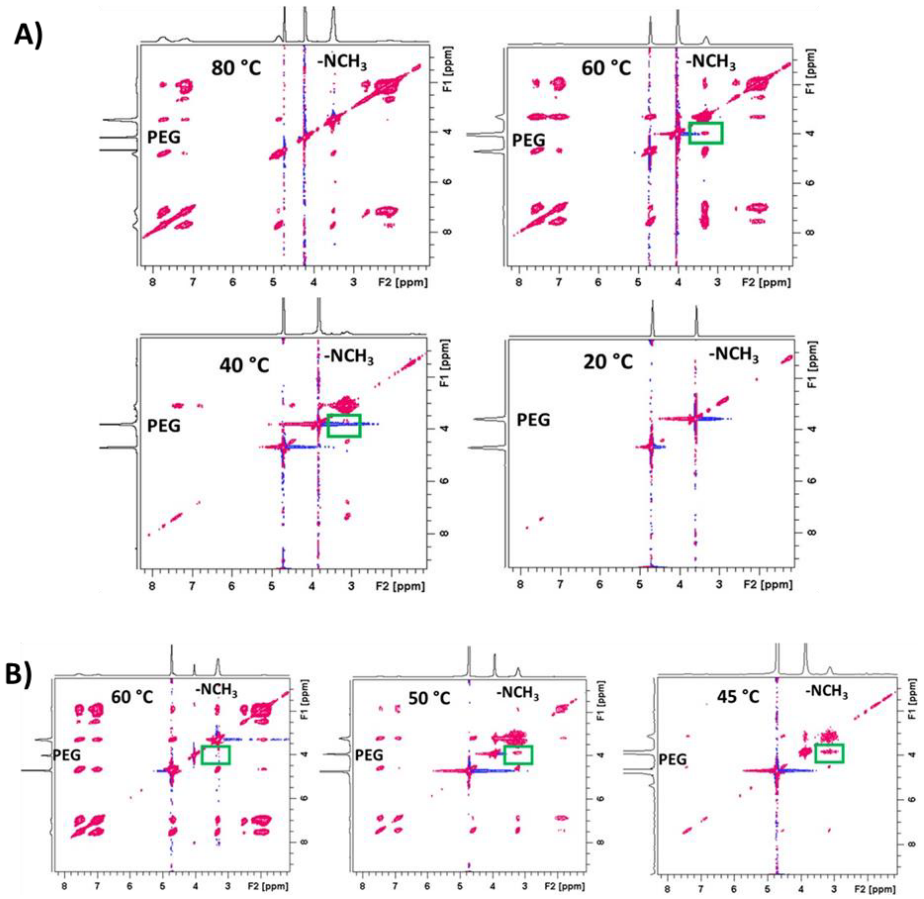

Figure 16 *^{1}H-^{1}H NOESY spectra at different temperatures. (A) VB-62 in D_2O with 150 mM LiOTf and (B) VB-270 in D_2O with 50 mM LiOTf. The cross-peaks of PEG and the cation are marked with green boxes.* [II]

To sum up, the stepwise phase separation of the copolymers is not only dependent on the salt concentration, but also on the molar mass of the cationic blocks. Upon cooling, VB_{62} copolymer phase separated below T_{cU} into large aggregates and then dispersed into smaller ones upon further cooling; this was not observed for VB_{172} or VB_{270}. Based on the findings, it is suggested that VB_{62} colloid particles are at low temperatures sterically stabilized with PEG chains, whereas in the dispersions of VB_{172} and VB_{270} the PEG chains are buried inside the cationic cores. Depending on the LiOTf concentration, VB_{81} copolymers show features of both high and low molar mass polymers. The interactions between ethylene glycol and charged units in the polymers may lead to complex phase separation.[56,147,148]

4.4 Syntheses of cationic particles via PISA

4.5.1 RAFT dispersion polymerization of PDAAM

The cationic sterically stabilized particles were synthesized via RAFT dispersion polymerization of DAAM at 70 °C using various macroCTAs 1-7 listed in Table 2. The

detailed list of dispersions obtained from various series with changing the reaction parameters such as target DP of PDAAM, salt and solids concentration are listed in the corresponding articles III, IV and supporting information. The polymerization kinetics of DAAM with targeting to DP 827 was followed in aqueous salt solutions (1M NaCl) using $PVBTMAC_{21}$ at 20 w/w %. From the NMR analysis, it was clear that the full conversion of DAAM was achieved in all cases within 1.5–3 h reaction time.

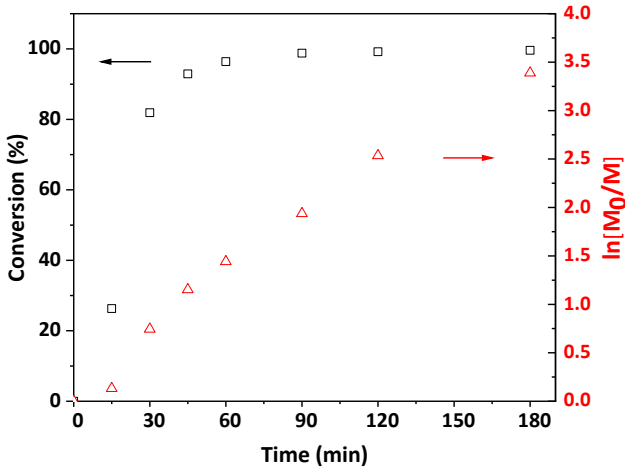

Figure 17 *Conversion of DAAM (black□) versus time and the corresponding semi logarithmic plot (red Δ) for the polymerization of DAAM with $PVBTMAC_{27}$ at 70 °C.* [III]

The DAAM conversions obtained in the polymerization of $PVBTMAC_{27}$-$PDAAM_{827}$ are plotted against time in Figure 17. The transparent reaction solutions turned turbid within few minutes of the polymerization. Due to the in situ self-assembly of copolymers, there is an increase in local concentration of monomers within the particles. Therefore, after a short initiation period, high monomer conversions were achieved within 60 min. The semilogarithmic plot in figure 17 shows that the rate of polymerization increased linearly after 15 min. The kinetics are consistent with those on nonionic copolymer systems of PDAAM and follow the typical RAFT dispersion polymerizations.[118,119] Similar kinetics were also observed for the polymerizations conducted with target DP 500 using other macroCTAs 3-7 (see table 2) at 15 w/w % solids.

4.5.2 Particles without salt

The dispersion polymerizations conducted in the salt-free solutions produced highly cationic particles. In the case of V_{21}-D_m, the hydrodynamic diameters of the particles increased with either increasing the target DP of the PDAAM or solids concentrations. The zeta potentials and electrophoretic mobilities showed the presence of particles with positively charged shells. However, TEM images showed that only spherical nanoparticles were obtained from salt-free dispersions (figure 18). With increasing solid content or DP of PDAAM, the diameters of the particles increased but no morphological change occurred. This is because of electrostatic repulsion in the particle shells, which inhibited the fusion of the spheres. Similar diblock copolymer systems have been reported earlier, only an increase in the diameters of spherical particles was observed under salt free conditions.[126,134]Also, only spherical particles were obtained when other cationic macroCTAs 2-7 were chain extended with DAAM in pure water.

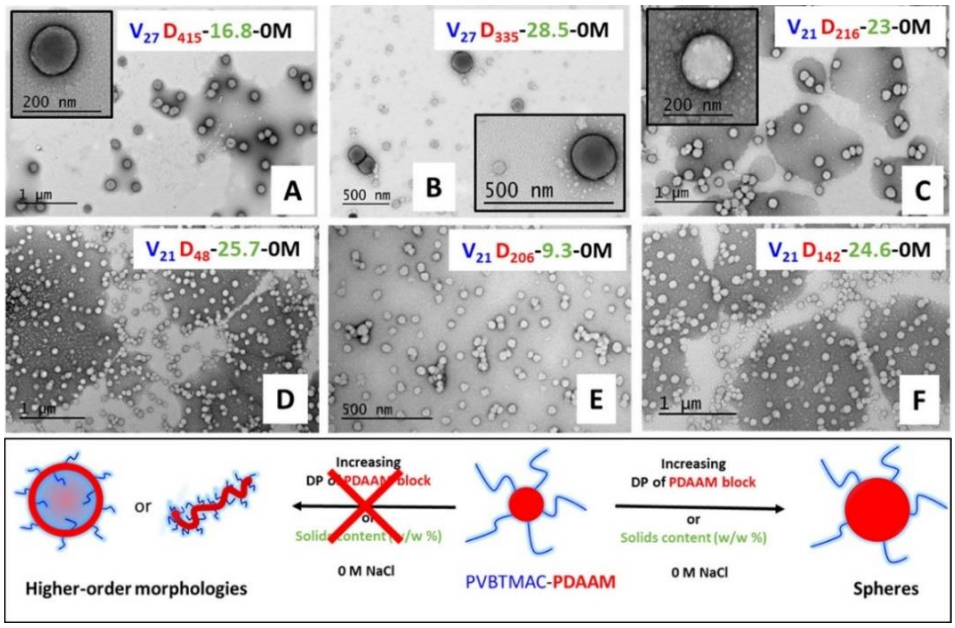

Figure 18 *TEM images of spherical nanoparticles obtained from the salt-free dispersions with varying DP of DAAM and total solids (w/w %, in green).* [III]

4.5.3 Morphological transition with salt

In the case of dispersions (V_{27}-D_{248}) obtained with styrene-based macroCTA ($PVBTMAC_{27}$), particle sizes increased with increasing the NaCl concentration. With TEM, particles with different morphologies were observed with changing the salt concentration in the polymerizations (figure 19). In 0.3 M salt, fused spheres were obtained. With increasing the salt concentration, the charge repulsions between the cationic stabilizers decrease as the ionic strength increases. With increasing the ionic ratio = [NaCl]/[Cp] from 4 to 8, or salt concentration from 0.5 to 1 M the particle morphologies were promoted to worm like structures. At ionic ratio 10 or above, a mixture of spheres and vesicles were observed. At low solids content (16.6 w/w%), vesicles and lamellar structures were obtained when 2 M NaCl was used in the polymerization (figure 19).

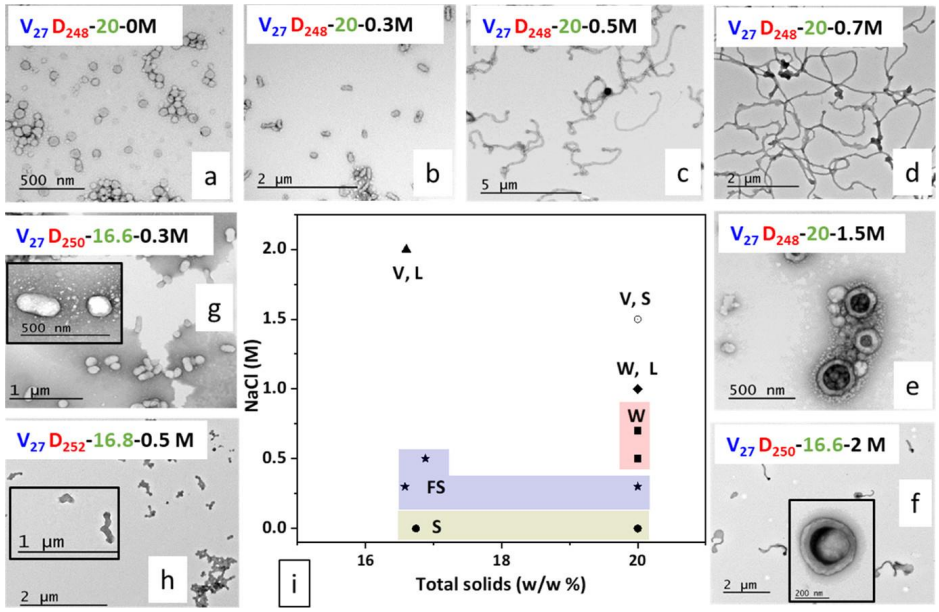

Figure 19 *TEM images and morphological phase diagram of particles obtained with varying the salt concentration and solids content 20 w/w % (a–e), and 16–17% (g,h,f). S = spheres(●), FS = fused spheres(★), W = worms(■), a mixed phase of lamellae and worms (W,L = ◆), a mixed phase of vesicles and spheres (V,S = ○) and a mixed phase of vesicles and lamellae (V,S = ▲).* [III]

The dispersion polymerizations were conducted with other macroCTAs (3-7 from table2) to construct the full morphological phase diagram (figure 20). The target DP of PDAAM 500 and solids content 15 w/w% were kept constant, changing the NaCl concentrations. Using the short styrenic macroCTA, $PVBTMAC_{24}$, only spherical particles were obtained with ionic ratio up to 12 (figure 20a). The morphological changes from spheres to fused spheres or cloudberry structures were observed with changing the ionic ratio to 16. However, no worm phase was observed. High ionic ratio 20 was required to induce the vesicular morphologies when using $PVBTMAC_{24}$ (figure 20d).

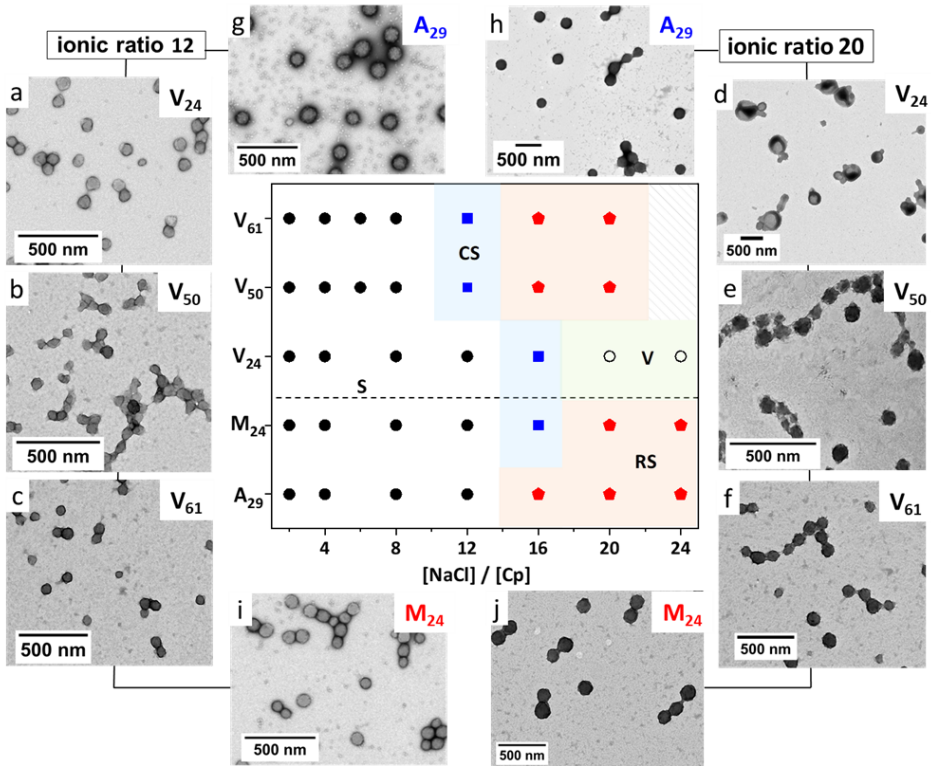

Figure 20 *TEM images of the particles obtained from the salt series using different macroCTAs. (a and d) V_{24}-D_{500}, (b and e) V_{50}-D_{500}, (c and f) V_{61}-D_{500}, (g and h) A_{29}-D_{500}, (i and j) M_{24}-D_{500}. The phase diagram of the particle morphologies at various ionic ratios. S= Spheres (●), CS= cloudberry structures (■) RS= raspberry structures (⬟) and V= vesicles (○).[Cp]= cationic repeating unit.* [IV]

Using long styrenic stabilizers, $PVBTMAC_{50}$ or $PVBTMAC_{61}$, the copolymers were mainly self-assembled to spherical particles at ionic ratio 8 or below when solids content was 15 w/w%. Further increasing the ionic ratio up to 12, the particle morphologies changed from the spheres to cloudberry structures (figure 20b and c). At high ionic ratios 16 or 20, raspberry structures were obtained from both V_{50}-D_{500} and $V_{61}D_{500}$ (figure 20e and f). Under TEM, the cloudberry particles consist of a low number of fused spheres. In the raspberries, the number of the spherical aggregated particles is higher but the spheres are smaller than those in the cloudberries.

The particles obtained with other macroCTAs, $PMOTAC_{24}$ and $PAMPTMAC_{29}$, followed a similar trend as long styrenic stabilizers. Only spheres were obtained with ionic ratio up to 12 (figure 20g and i). With increasing the ionic ratio, the particle morphology changed from spheres to cloudberries and/or raspberries (figure 20h and j). At ionic ratio 24, dense raspberry-like particles were obtained when using acrylamide macroCTA. Similar raspberries but smaller in size were formed for $M_{24}D_{500}$.

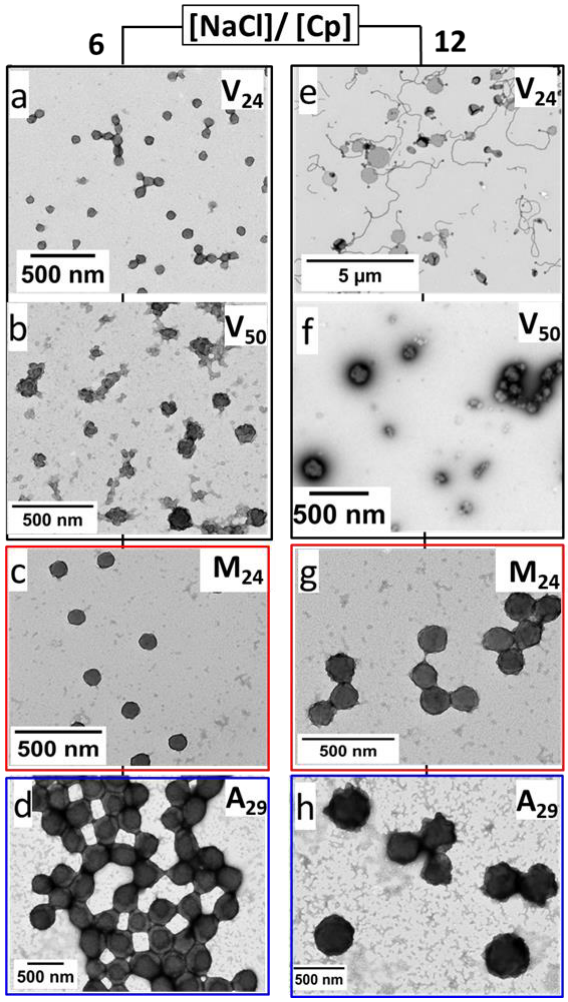

Figure 21 *TEM images of the particles obtained at 20 w/w % using ionic ratios [NaCl]/ [Cp] 6 and 12.*[IV]

TEM images of the particles obtained at 20 w/w % with low salt concentrations are shown in figure 21. At lower ionic ratio 6, cloudberry-like structures were observed for the particles obtained with styrene based macroCTAs (figure 21a and b). With increasing the salt concentration, the particle morphology changed to a mixed phase of worms, lamella and vesicles when using the short styrenic macroCTA (figure 21e). Only berry-like structures were obtained using long styrenic macroCTA (figure 21f). Similar morphological changes were observed in methacrylate based $M_{24}D_{500}$ particles with changing the ionic ratio (figure 21c and g). The particles obtained with acrylamide-based CTA resembled vesicular structures at both ionic ratios (figure 21d and h).

4.5.4 Effect of DP of PDAAM

To study the effect of DP of PDAAM, several polymerizations of DAAM were conducted in aqueous salt solutions using $PVBTMAC_{27}$ while keeping NaCl (1 M) and solids concentration (20 w/w%) constant. With low target DP of PDAAM, only spherical particles were obtained.

As is typical in PISA, fused spheres or worm-like structures started to build up with increasing the target DP. When the second block DP was targeted to above 300, the particle morphology changed from long worm structures to a mixed phase of vesicles and lamella (figure 22). Similar interconnected lamella or vesicles were observed for copolymers with nonionic stabilizers or ionic copolymers of styrene.[78,122,149]

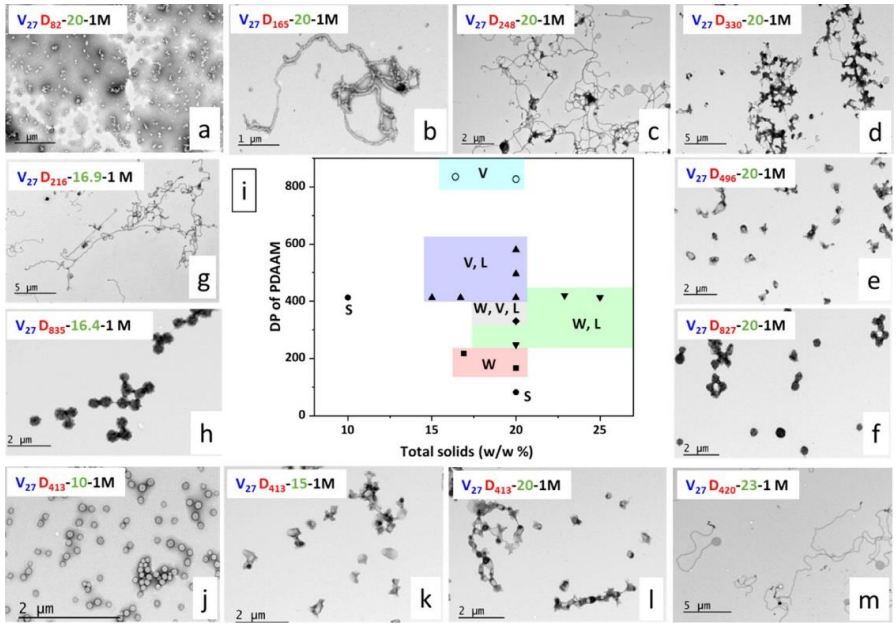

Figure 22 *TEM micrographs of nano-objects obtained in the presence of NaCl (1 M) with different target DP of PDAAM and solids. (a–f) Target DP increases from 82 to 827 at 20 w/w %; (g,h) target DP 216 and 835 at low solids w/w %; (j–m) different solid contents w/w %; and (i) phase diagram of particles.*[III]

With high target DP of PDAAM > 800, particle morphology changed to pure vesicular structure, which looked like dense raisins under FESEM. Similar morphologies were obtained when the solids content was kept low, 16.4 w/w% (figure 22 h and f). With target DP 413, spherical particles were obtained at low solids content. Targeting the same DP of PDAAM, the particle morphology changed from sphere to lamella or mixed phase of lamella and vesicles or worms when increasing the solids content from 10 to 23 w/w% (figure 22j-m).

4.5.5 Thermoresponsive behavior of particles

Triflate ions induce thermoresponsive behavior in aqueous polycations. Properties of few colloids with different particle compositions were investigated. The cloudiness increased when triflate ions were introduced to $V_{21}D_{48}$ dispersions. Normalized transmittance curves obtained with different LiOTf concentrations are shown in figure 25A and B. Upon cooling, the particles undergo phase separation below 65 °C when the ionic ratio [LiOTf]/[VBTMAC]=10 was used. With low triflate concentrations, the particles either underwent weak phase transitions, or phase separation took place in two steps upon cooling. The transmittance heating curves confirmed the disintegration of the particle aggregates. Upon heating, the dispersions became less cloudy as the solubilities of the cationic shells changed.

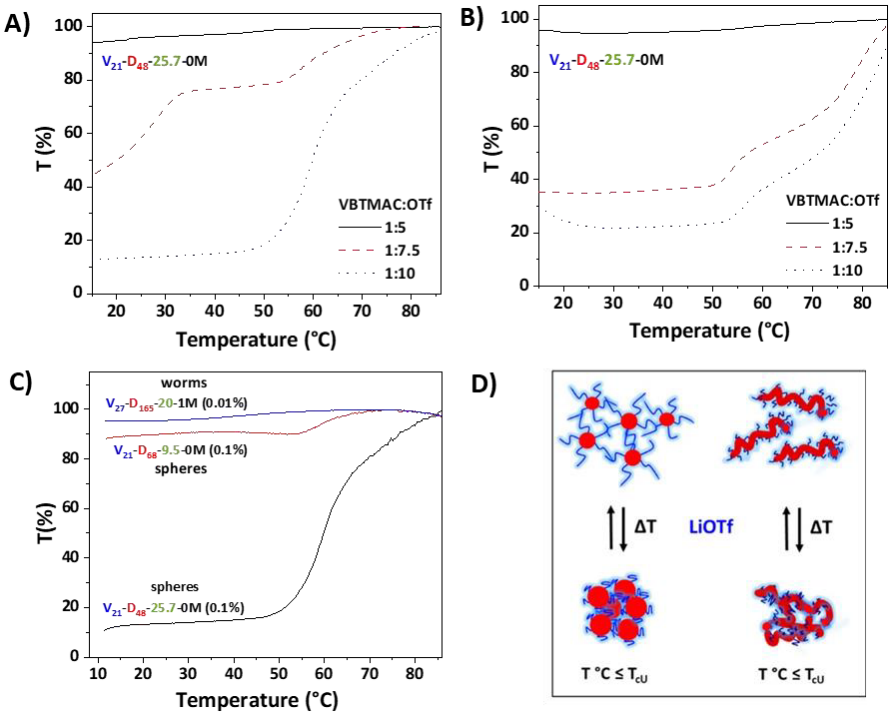

Figure 23 *Particles synthesized in salt-free solutions. A) Normalized transmittance cooling curves for spherical nanoparticles of V_{21}-D_{48} (0.1 w/w %) in aqueous triflate solutions with different cation/anion ratios. (B) Corresponding heating curves. C) Particles with different morphologies in aqueous triflate solutions with a cation/anion ratio of 1:10. D) Cartoon of thermoresponsive behavior of the particles.* [III]

The phase separation behavior was different in the particles with different core block lengths. Upon cooling, spheres with small cores showed considerable changes in transmittance. Particles either with large cores or with worm morphologies showed weak transmittance changes upon cooling (figure 23C).

4.5.6 PISA in aqueous triflate solutions

As discussed above, the solubility of cationic macroCTAs can be changed with LiOTf ions. A series of dispersion polymerizations were conducted in aqueous LiOTf solutions using macroCTAs 3-7. In the reaction mixtures LiOTf concentration was adjusted respective to the cationic repeating units. First, the ionic ratio [LiOTf]/[Cp]=1 and solids content (15 w/w%) was kept constant while targeting the DP of PDAAM 500. The cloudy dispersions obtained at 70 °C using styrene-based macroCTAs formed free-standing gels upon cooling. With TEM, a mixture of spheres and/or fused spheres were observed from hot dispersions (figure 24a, c, and e). The particle morphology changed to either fused aggregates or worm-like networks in the cooled dispersions (figure 24b, d, and f). Using high ionic ratios in the polymerization led to completely precipitated dispersions at 70 °C. TEM depicts only spherical particles from the dispersions obtained with other macroCTAs $PMOTAC_{24}$ and $PAMPTMAC_{29}$.

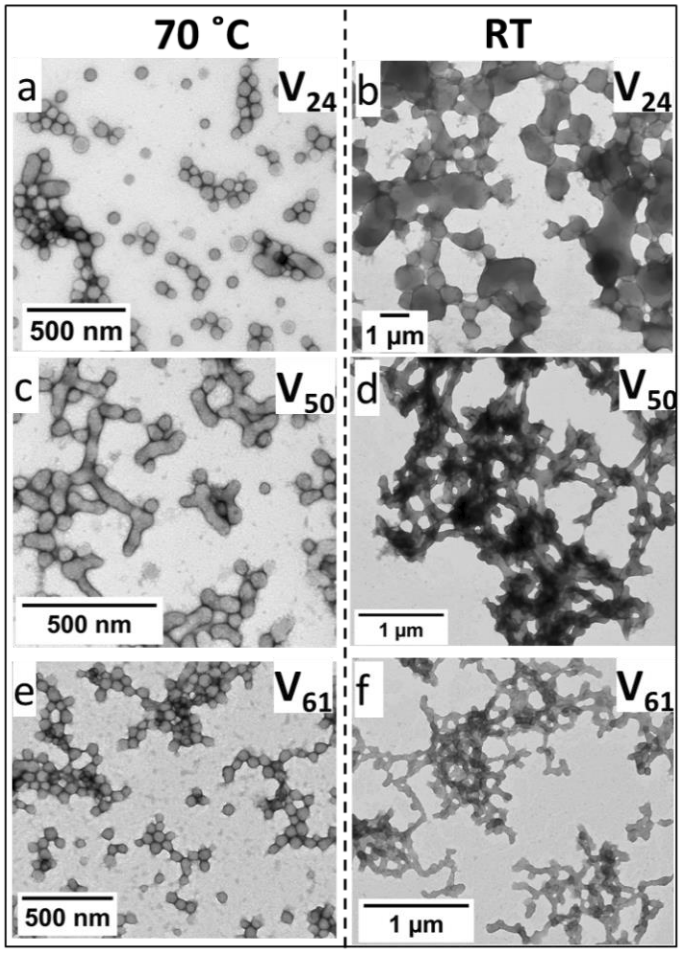

Figure 24 *TEM micrographs of the particles from V_n-D_{500} dispersions obtained in LiOTf solutions at 15 w/w % with ionic ratio [LiOTf]/[Cp] =1 . TEM samples were collected from both hot (from 70 °C, left) and cooled (at room temperature, right) dispersions.* [IV]

With increasing the solids content up to 20 w/w% the morphologies changed from fused spheres to a mixture of spheres and vesicles at elevated temperatures in the case of the short styrenic macroCTA. When cooling the dispersions to RT, the morphology changed to fused aggregates or vesicles (figure 25a and b). The vesicles obtained at 20 w/w% contained small lumens (see figure 25a), indicating the membrane had grown inwards to the particles, as observed in other copolymer systems.[150–152] In the case of long styrenic macroCTAs, fused spheres were observed from the hot dispersions obtained with 20 w/w%. However, the copolymers phase separated completely when cooled to room temperature. At high solids content, only spherical particles were obtained with $PMOTAC_{24}$, and $PAMPTMAC_{29}$. No morphological transitions were observed upon cooling (figure 25c-f).

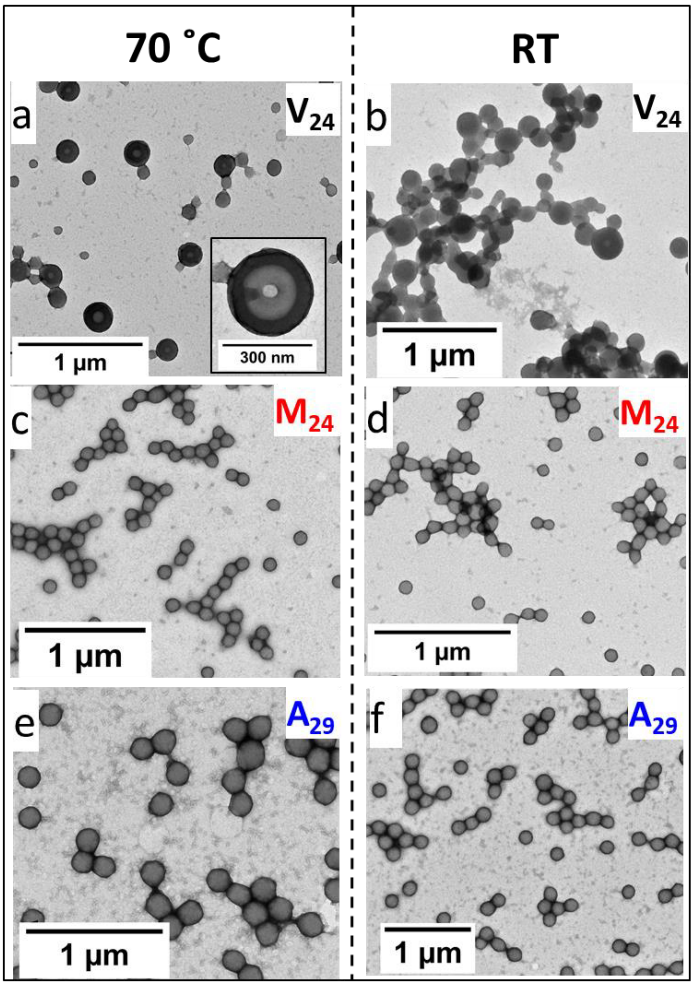

Figure 25 *TEM micrographs of the particles obtained in LiOTf solutions with ionic ratio [LiOTf]/[Cp]=1 at 20 w/w %. DP of PDAAM was 500. The samples were collected from both hot (70 °C, left) and cooled (room temperature, right) dispersions.* [IV]

In the presence of equal amounts of triflate ions (as in figure 25), PAMPTAMC and PMOTAC are less hydrophobic than PVBTMAC. The fusion of spheres mainly took place when styrene-based macroCTAs were used, because the styrenic polycations undergo UCST-type phase separation upon cooling. The shrinkage of the cationic shells rapidly led to morphological transitions upon cooling. Several copolymer systems undergo order-order morphological transitions with changing temperature, however, hours or days can take place for full transitions.[137,153–155] As the solubilities of PMOTAC and PAMPTAMC were not influenced by triflate ions, no particle fusion took place in their particles.

5 Conclusions

The thesis discusses the aqueous solution properties of polycations, diblock copolymers and their particles.

The styrene-based polycations bearing triflate counterions underwent temperature dependent phase separation in aqueous LiOTf solutions. A sufficient amount of triflate ions was needed to induce an UCST type phase transition. The colloidal stability of the phase separated aggregates mainly depended on the concentrations of salt and polymer. The polycations with chloride counterions showed considerable changes in the phase separation behavior in constant LiOTf concentration. The cloud points shifted to higher temperatures with increasing the molar mass of PVBTMAC. PMOTAC and PAMPTAMC did not phase separate under the same conditions, but higher LiOTf concentrations or molar masses were needed compared to styrenic ones to induce the UCST.[53]

The diblock copolymers, PEG-PVBTMA-OTf with different lengths of the cationic blocks were synthesized via controlled RAFT polymerization. The phase separation of PVBTMA-OTf took place in a stepwise manner in aqueous triflate solutions when it was covalently bound to PEG. Upon cooling, the solutions of the copolymer with short cationic blocks phase separated below T_{cU}, and then became partially clear upon further cooling below T_{cL}. VB_{81} behaved similarly to VB_{62} in certain LiOTf concentrations. Below T_{cL}, the phase-separated aggregates were sterically stabilized with PEG chains. The polymers with long polycation blocks, VB_{172} and VB_{270}, phase separated in one process within a narrow temperature range. The particles built up were stabilized by the charges of the polycation, whereas the PEG blocks were buried in the cationic cores.

The polycation macroCTAs were chain extended with DAAM via RAFT polymerization in aqueous solutions. Due to the charge repulsions in the cationic shells, only spherical particles were obtained in pure water. In the presence of NaCl, the fusion of the particles took place. With increasing the ionic ratio [NaCl]/[Cp], the morphological transition from spheres to fused aggregates or worms to vesicles were observed when short styrenic macroCTAs were used. Either with long styrenic stabilizers or with other macroCTAs PMOTAC and PAMPTMAC, the particle morphologies changed from spheres to raspberry structures with increasing the salt concentration.

The particles $V_{21}D_{48}$ obtained from salt free dispersions were shown to undergo UCST type phase separation in aqueous triflate solutions. The polymerizations were also conducted in aqueous LiOTf solutions. Fused spheres were obtained when the styrene-based macroCTAs were used. When increasing the solids content, the copolymers with short styrenic CTAs formed vesicles with thick bilayers. The particles underwent morphological transitions with changing the temperature. On the other hand, triflate ions did not affect the morphology of particles obtained with PMOTAC and PAMPTAC macroCTAs.

Overall, it has been shown that using triflate ions the polycations can be turned thermoresponsive. Covalent linkage of hydrophilic blocks to the thermoresponsive polycations enhances the stability of the particles. Using styrenic polycations as sole steric stabilizers in PISA, a full morphological window of particles can be obtained in saline solutions. The styrene-based cationic particles undergo an UCST type phase separation. Further, order-order or morphological transitions of the particles can be achieved using triflate ions in PISA.

6 References

(1) Dobrynin, A.V. Solutions of Charged Polymers, in *Polymer Science: A Comprehensive Reference*, Edited by Matyjaszewski, K.; Möller, M., Elsevier, **2012**

(2) Muthukumar, M. 50th Anniversary Perspective: A Perspective on Polyelectrolyte Solutions. Macromolecules **2017**, 50 (24), 9528–9560.

(3) Dobrynin, A. V. Polyelectrolytes: On the Doorsteps of the Second Century. Polymer **2020**, 202, 122714.

(4) Kudaibergenov, S. E. Recent Advances in the Study of Synthetic Polyampholytes in Solutions. Adv. Polym. Sci. **1999**, 144, 115–197.

(5) Hess, M.; Jones, R. G.; Kahovec, J.; Kitayama, T.; Kratochvíl, P.; Kubisa, P.; Mormann, W.; Stepto, R. F. T.; Tabak, D.; Vohlídal, J.; Wilks, E. S. Terminology of Polymers Containing Ionizable or Ionic Groups and of Polymers Containing Ions (IUPAC Recommendations 2006). Pure Appl. Chem. **2006**, 78 (11), 2067–2074.

(6) Wilts, E. M.; Herzberger, J.; Long, T. E. Addressing Water Scarcity: Cationic Polyelectrolytes in Water Treatment and Purification. Polym. Int. **2018**, 67 (7), 799–814.

(7) Papagiannopoulos, A. Current Research on Polyelectrolyte Nanostructures: From Molecular Interactions to Biomedical Applications. Macromol 2021, **2021**, 1 (2), 155–172.

(8) Samal, S. K.; Dash, M.; Vlierberghe, S. Van; Kaplan, D. L.; Chiellini, E.; Blitterswijk, C. van; Moroni, L.; Dubruel, P. Cationic Polymers and Their Therapeutic Potential. Chem. Soc. Rev. **2012**, 41 (21), 7147–7194.

(9) Moroson, H.; Rotman, M. Biomedical Applications of Polycations. Polyelectrolytes their Appl. **1975**, 187–195.

(10) Katchalsky, A.; Eisenberg, H. Molecular Weight of Polyacrylic and Polymethacrylic Acid. J. Polym. Sci. **1951**, 6 (2), 145–154.

(11) Manning, G. S. Counterion Condensation Theory Constructed from Different Models. Phys. A Stat. Mech. its Appl. **1996**, 231 (1–3), 236–253.

(12) Brilliantov, N. V; Kuznetsov, D. V; Klein, R. Chain Collapse and Counterion Condensation in Dilute Polyelectrolyte Solutions. **1998**.

(13) Raphael, E.; Joanny, J. F. Annealed and Quenched Polyelectrolytes. Europhys. Lett. **1990**, 13 (7), 623.

(14) Lee, C. L.; Muthukumar, M. Phase Behavior of Polyelectrolyte Solutions with Salt. J. Chem. Phys. **2009**, 130 (2).

(15) Liu, S.; Ghosh, K.; Muthukumar, M. Polyelectrolyte Solutions with Added Salt: A Simulation Study. J. Chem. Phys. **2003**, 119 (3), 1813–1823.

(16) Ghosh, S.; Vemparala, S. Kinetics of Charged Polymer Collapse in Poor Solvents. J. Phys. Condens. Matter **2021**, 34 (4), 045101.

(17) Tom, A. M.; Vemparala, S.; Rajesh, † R; Brilliantov, N. V. Mechanism of Chain Collapse of Strongly Charged Polyelectrolytes. **2016**.

(18) Sabbagh, I.; Delsanti, M. Solubility of Highly Charged Anionic Polyelectrolytes in Presence of Multivalent Cations: Specific Interaction Effect. Eur. Phys. J. E **2000**, 1, 75–86.

(19) Bütün, V.; Armes, S. P.; Billingham, N. C. Synthesis and Aqueous Solution Properties of Near-Monodisperse Tertiary Amine Methacrylate Homopolymers and Diblock Copolymers. Polymer **2001**, 42 (14), 5993–6008.

(20) Plamper, F. A.; Ruppel, M.; Schmalz, A.; Borisov, O.; Ballauff, M.; Müller, A. H. E. Tuning the Thermoresponsive Properties of Weak Poly Electrolytes: Aqueous Solutions of Star-Shaped and Linear Poly(N,N-Dimethylaminoethyl Methacrylate). Macromolecules **2007**, 40 (23), 8361–8366.

(21) Karjalainen, E.; Aseyev, V.; Tenhu, H. Influence of Hydrophobic Anion on Solution Properties of PDMAEMA. Macromolecules **2014**, 47 (6), 2103–2111.

(22) Thavanesan, T.; Herbert, C.; Plamper, F. A. Insight in the Phase Separation Peculiarities of Poly(Dialkylaminoethyl Methacrylate)S. Langmuir **2014**, 30 (19), 5609–5619.

(23) Kou, R.; Zhang, J.; Wang, T.; Liu, G. Interactions between Polyelectrolyte Brushes and Hofmeister Ions: Chaotropes versus Kosmotropes. Langmuir **2015**, 31 (38), 10461–10468.

(24) Bibi, I.; Siddiq, M. Conformational Transition of Poly (Vinylbenzyltrimethylammonium Chloride) (PVBTMAC) Brush in the Presence of Hofmeister Anions. J. Polym. Res. **2012**, 19 (9), 1–5.

(25) Itaya, T.; Ueda, K.; Ochiai, H.; Imamura, A. Binding of Hydrophobic Counterions by Polyelectrolyte and Their Hydrophobic Association around Polyion. Polym. J. **1993**, 25 (6), 545–552.

(26) Zimerman, O. E.; Cosa, J. J.; Previtali, C. M. Binding of Ionic Pyrene Derivatives to Polyelectrolytes. A Uv Absorption and Fluorescence Study. http://dx.doi.org/10.1080/10601329409349763 **2008**, 31 (7), 859–872.

(27) Karjalainen, E.; Chenna, N.; Laurinmaeki, P.; Butcher, S. J.; Tenhu, H. Diblock Copolymers Consisting of a Polymerized Ionic Liquid and Poly(N-Isopropylacrylamide). Effects of PNIPAM Block Length and Counter Ion on Self-Assembling and Thermal Properties. Polym. Chem. **2013**, 4, 1014–1024.

(28) Texter, J. Anion Responsive Imidazolium-Based Polymers. Macromol. Rapid Commun. **2012**, 33 (23), 1996–2014.

(29) Vijayakrishna, K.; Mecerreyes, D.; Gnanou, Y.; Taton, D. Polymeric Vesicles and Micelles Obtained by Self-Assembly of Ionic Liquid-Based Block Copolymers Triggered by Anion or Solvent Exchange. Macromolecules **2009**, 42 (14), 5167–5174.

(30) Vijayakrishna, K.; Jewrajka, S. K.; Ruiz, A.; Marcilla, R.; Pomposo, J. A.; Mecerreyes, D.; Taton, D.; Gnanou, Y. Synthesis by RAFT and Ionic Responsiveness of Double Hydrophilic Block Copolymers Based on Ionic Liquid Monomer Units. Macromolecules **2008**, 41 (17), 6299–6308.

(31) Aseyev, V. O.; Tenhu, H.; Klenin, S. I. Collapse of Poly(Methacryloylethyl Trimethylammonium Methylsulfate) on Addition of Acetone into an Aqueous Solution. Polymer **1999**, 40, 1173-1180.

(32) Aseyev, V. O.; Tenhu, H.; Klenin, S. I. Contraction of a Polyelectrolyte upon Dilution. Light-Scattering Studies on a Polycation in Saltless Water−Acetone Mixtures.

Macromolecules **1998**,

(33) Aseyev, V.; Tenhu, H.; Winnik, F. M. Non-Ionic Thermoresponsive Polymers in Water; **2010**; pp 29–89.

(34) Seuring, J.; Agarwal, S. Polymers with Upper Critical Solution Temperature in Aqueous Solution. Macromol. Rapid Commun. **2012**, 33 (22), 1898–1920.

(35) Schulz, D. N.; Peiffer, D. G.; Agarwal, P. K.; Larabee, J.; Kaladas, J. J.; Soni, L.; Handwerker, B.; Garner, R. T. Phase Behaviour and Solution Properties of Sulphobetaine Polymers. Polymer **1986**, 27 (11), 1734–1742.

(36) Niskanen, J.; Vapaavuori, J.; Pellerin, C.; Winnik, F. M.; Tenhu, H. Polysulfobetaine-Surfactant Solutions and Their Use in Stabilizing Hydrophobic Compounds in Saline Solution. Polymer **2017**, 127, 77–87.

(37) Lewoczko, E. M.; Wang, N.; Lundberg, C. E.; Kelly, M. T.; Kent, E. W.; Wu, T.; Chen, M. L.; Wang, J. H.; Zhao, B. Effects of N-Substituents on the Solution Behavior of Poly(Sulfobetaine Methacrylate)s in Water: Upper and Lower Critical Solution Temperature Transitions. ACS Appl. Polym. Mater. **2021**, 3 (2), 867–878.

(38) Niskanen, J.; Tenhu, H. How to Manipulate the Upper Critical Solution Temperature (UCST)? Polym. Chem. **2017**, 8 (1), 220–232.

(39) Kohno, Y.; Saita, S.; Men, Y.; Yuan, J.; Ohno, H. Thermoresponsive Polyelectrolytes Derived from Ionic Liquids. Polym. Chem. **2015**, 6 (12), 2163–2178.

(40) Kohno, Y.; Ohno, H.; Kohno, Y.; Ohno, H. Key Factors to Prepare Polyelectrolytes Showing Temperature-Sensitive Lower Critical Solution Temperature-Type Phase Transitions in Water. Aust. J. Chem. **2011**, 65 (1), 91–94.

(41) Deguchi, Y.; Kohno, Y.; Ohno, H.; Deguchi, Y.; Kohno, Y.; Ohno, H. Design of Ionic Liquid-Derived Polyelectrolyte Gels Toward Reversible Water Absorption/Desorption System Driven by Small Temperature Change. Aust. J. Chem. **2014**, 67 (11), 1666–1670.

(42) Men, Y.; Schlaad, H.; Yuan, J. Cationic Poly(Ionic Liquid) with Tunable Lower Critical Solution Temperature-Type Phase Transition. ACS Macro Lett. **2013**, 2 (5), 456–459.

(43) Okafuji, A.; Kohno, Y.; Ohno, H.; Okafuji, A.; Kohno, Y.; Ohno, H. Thermoresponsive Poly(Ionic Liquid)s in Aqueous Salt Solutions: Salting-Out Effect on Their Phase Behavior and Water Absorption/Desorption Properties. Macromol. Rapid Commun. **2016**, 37 (14), 1130–1134.

(44) Ju, C.; Park, C.; Kim, T.; Kang, S.; Kang, H. Thermo-Responsive Draw Solute for Forward Osmosis Process; Poly(Ionic Liquid) Having Lower Critical Solution Temperature Characteristics. RSC Adv. **2019**, 9 (51), 29493–29501.

(45) Yoshimitsu, H.; Kanazawa, A.; Kanaoka, S.; Aoshima, S. Well-Defined Polymeric Ionic Liquids with an Upper Critical Solution Temperature in Water. Macromolecules **2012**, 45 (23), 9427–9434.

(46) Biswas, Y.; Maji, T.; Dule, M.; Mandal, T. K. Tunable Doubly Responsive UCST-Type Phosphonium Poly(Ionic Liquid): A Thermosensitive Dispersant for Carbon Nanotubes. Polym. Chem. **2016**, 7 (4), 867–877.

(47) Ge, C.; Liu, S.; Liang, C.; Ling, Y.; Tang, H. Synthesis and UCST-Type Phase Behavior of α-Helical Polypeptides with Y-Shaped and Imidazolium Pendants. Polym.

Chem. **2016**, 7 (38), 5978–5987.

(48) Zhu, M.; Liu, W.; Xiao, J.; Ling, Y.; Tang, H. Synthesis and UCST-Type Phase Behaviors of OEGylated Random Copolypeptides in Alcoholic Solvents. J. Polym. Sci. Part A Polym. Chem. **2016**, 54 (21), 3444–3453.

(49) Zheng, Z.; Zhang, L.; Ling, Y.; Tang, H. Triblock Copolymers Containing UCST Polypeptide and Poly(Propylene Glycol): Synthesis, Thermoresponsive Properties, and Modification of PVA Hydrogel. Eur. Polym. J. **2019**, 115, 244–250.

(50) Li, M.; He, X.; Ling, Y.; Tang, H. Dual Thermoresponsive Homopolypeptide with LCST-Type Linkages and UCST-Type Pendants: Synthesis, Characterization, and Thermoresponsive Properties. Polymer **2017**, 132, 264–272.

(51) Niskanen, J.; Wu, C.; Ostrowski, M.; Fuller, G. G.; Hietala, S.; Tenhu, H. Thermoresponsiveness of PDMAEMA. Electrostatic and Stereochemical Effects. Macromolecules **2013**, 46 (6), 2331–2340.

(52) Cao, X.; An, Z.; Cao, X.; An, Z. RAFT Synthesis in Water of Cationic Polyelectrolytes with Tunable UCST. Macromol. Rapid Commun. **2015**, 36 (23), 2107–2110.

(53) Karjalainen, E.; Aseyev, V.; Tenhu, H. Counterion-Induced UCST for Polycations. Macromolecules **2014**, 47 (21), 7581–7587.

(54) Karjalainen, E.; Suvarli, N.; Tenhu, H. Thermoresponsive Behavior of Poly[Trialkyl-(4-Vinylbenzyl)Ammonium] Based Polyelectrolytes in Aqueous Salt Solutions. Polym. Chem. **2020**, 11 (36), 5870–5883.

(55) Longenecker, R.; Mu, T.; Hanna, M.; Burke, N. A. D.; Stöver, H. D. H. Thermally Responsive 2-Hydroxyethyl Methacrylate Polymers: Soluble-Insoluble and Soluble-Insoluble-Soluble Transitions. Macromolecules **2011**, 44 (22), 8962–8971.

(56) Zhang, Y.; Tang, H.; Wu, P. Multiple Interaction Regulated Phase Transition Behavior of Thermo-Responsive Copolymers Containing Cationic Poly(Ionic Liquid)S. Phys. Chem. Chem. Phys. **2017**, 19 (45), 30804–30813.

(57) Jana, S.; Biswas, Y.; Anas, M.; Saha, A.; Mandal, T. K. Poly[Oligo(2-Ethyl-2-Oxazoline)Acrylate]-Based Poly(Ionic Liquid) Random Copolymers with Coexistent and Tunable Lower Critical Solution Temperature- and Upper Critical Solution Temperature-Type Phase Transitions. Langmuir **2018**, 34 (42), 12653–12663.

(58) Karjalainen, E.; Aseyev, V.; Tenhu, H. Upper or Lower Critical Solution Temperature, or Both? Studies on Cationic Copolymers of N-Isopropylacrylamide. Polym. Chem. **2015**, 6 (16), 3074–3082.

(59) Yu, R.; Tauer, K. From Particles to Stabilizing Blocks – Polymerized Ionic Liquids in Aqueous Heterophase Polymerization. Polym. Chem. **2014**, 5 (19), 5644–5655.

(60) Wang, Z.; Lai, H.; Wu, P. Influence of PIL Segment on Solution Properties of Poly(N-Isopropylacrylamide)-b-Poly(Ionic Liquid) Copolymer: Micelles, Thermal Phase Behavior and Microdynamics. Soft Matter **2012**, 8 (46), 11644–11653.

(61) Tauer, K.; Weber, N.; Texter, J. Core–Shell Particle Interconversion with Di-Stimuli-Responsive Diblock Copolymers. Chem. Commun. **2009**, 40, 6065.

(62) Mori, H.; Yanagi, M.; Endo, T. RAFT Polymerization of N-Vinylimidazolium Salts and Synthesis of Thermoresponsive Ionic Liquid Block Copolymers. Macromolecules **2009**, 42 (21), 8082–8092.

(63) Han, X.; Zhang, X.; Yin, Q.; Hu, J.; Liu, H.; Hu, Y. Thermoresponsive Diblock Copolymer with Tunable Soluble-Insoluble and Soluble-Insoluble-Soluble Transitions. Macromol. Rapid Commun. **2013**, 34 (7), 574–580.

(64) Kim, B.; Kwon, M.; Mohanty, A. K.; Cho, H. Y.; Paik, H.-J.; Kim, B.; Kwon, M.; Mohanty, A. K.; Cho, H. Y.; Paik, H.-J. LCST and UCST Transition of Poly(DMAEMA-b-MEO2MA) Copolymer in KHP Buffer. Macromol. Chem. Phys. **2021**, 222 (2), 2000330.

(65) Israelachvili, J. N.; Mitchell, D. J.; Ninham, B. W. Theory of Self-Assembly of Lipid Bilayers and Vesicles. BBA - Biomembr. **1977**, 470 (2), 185–201.

(66) Zhulina, E. B.; Borisov, O. V. Theory of Block Polymer Micelles: Recent Advances and Current Challenges. Macromolecules. **2012**, 45 (11), 4429–4440.

(67) Mai, Y.; Eisenberg, A. Self-Assembly of Block Copolymers. Chem. Soc. Rev. **2012**, 41 (18), 5969–5985.

(68) Bates, F. S.; Fredrickson, G. H. Block Copolymers—Designer Soft Materials. Phys. Today **2008**, 52 (2), 32.

(69) Doncom, K. E. B.; Blackman, L. D.; Wright, D. B.; Gibson, M. I.; O'Reilly, R. K. Dispersity Effects in Polymer Self-Assemblies: A Matter of Hierarchical Control. Chem. Soc. Rev.*,* **2017**, 46, 4119-4134.

(70) Dionzou, M.; Morère, A.; Roux, C.; Lonetti, B.; Marty, J. D.; Mingotaud, C.; Joseph, P.; Goudounèche, D.; Payré, B.; Léonetti, M.; Mingotaud, A. F. Comparison of Methods for the Fabrication and the Characterization of Polymer Self-Assemblies: What Are the Important Parameters? Soft Matter **2016**, 12 (7), 2166–2176.

(71) Mai, Y.; Eisenberg, A. Self-Assembly of Block Copolymers. Chem. Soc. Rev. **2012**, 41 (18), 5969.

(72) Borisov, O. V.; Zhulina, E. B. Morphology of Micelles Formed by Diblock Copolymer with a Polyelectrolyte Block. Macromolecules **2003**, 36 (26), 10029–10036.

(73) Moffitt, M.; Khougaz, K.; Eisenberg, A. Micellization of Ionic Block Copolymers. Acc. Chem. Res. **1996**, 29 (2), 95–102.

(74) Lysenko, E. A.; Bronich, T. K.; Slonkina, E. V.; Eisenberg, A.; Kabanov, V. A.; Kabanov, A. V. Block Ionomer Complexes with Polystyrene Core-Forming Block in Selective Solvents of Various Polarities. 1. Solution Behavior and Self-Assembly in Aqueous Media. Macromolecules **2002**, 35 (16), 6351–6361.

(75) Gao, Z.; Varshney, S. K.; Wong, S.; Eisenberg, A. Block Copolymer "Crew-Cut" Micelles in Water. Macromolecules **1994**, 27 (26), 7923–7927.

(76) Zhang, L.; Eisenberg, A. Morphogenic Effect of Added Ions on Crew-Cut Aggregates of Polystyrene-b-Poly(Acrylic Acid) Block Copolymers in Solutions. Macromolecules **1996**, 29 (27), 8805–8815.

(77) Ho, C. S.; Kim, J. W.; Weitz, D. A. Microfluidic Fabrication of Monodisperse Biocompatible and Biodegradable Polymersomes with Controlled Permeability. J. Am. Chem. Soc. **2008**, 130 (29), 9543–9549.

(78) He, W. D.; Sun, X. L.; Wan, W. M.; Pan, C. Y. Multiple Morphologies of PAA-b-PSt Assemblies throughout RAFT Dispersion Polymerization of Styrene with PAA Macro-CTA. Macromolecules **2011**, 44 (9), 3358–3365.

(79) Wan, W.; Pan, C. One-Pot Synthesis of Polymeric Nanomaterials via RAFT Dispersion Polymerization Induced Self-Assembly and Re-Organization. **2010**, 1475–1484.

(80) Penfold, N. J. W.; Yeow, J.; Boyer, C.; Armes, S. P. Emerging Trends in Polymerization-Induced Self-Assembly. ACS Macro Lett. **2019**, 8 (8), 1029–1054.

(81) Ferguson, C. J.; Hughes, R. J.; Nguyen, D.; Pham, B. T. T.; Gilbert, R. G.; Serelis, A. K.; Such, C. H.; Hawkett, B. S. Ab Initio Emulsion Polymerization by RAFT-Controlled Self-Assembly. Macromolecules **2005**, 38 (6), 2191–2204.

(82) Ferguson, C. J.; Hughes, R. J.; Pham, B. T. T.; Hawkett, B. S.; Gilbert, R. G.; Serelis, A. K.; Such, C. H. Effective Ab Initio Emulsion Polymerization under RAFT Control. Macromolecules **2002**, 35 (25), 9243–9245.

(83) Rieger, J.; Stoffelbach, F.; Bui, C.; Alaimo, D.; Jérôme, C.; Charleux, B. Amphiphilic Poly(Ethylene Oxide) Macromolecular RAFT Agent as a Stabilizer and Control Agent in Ab Initio Batch Emulsion Polymerization. Macromolecules **2008**, 41 (12), 4065–4068.

(84) Li, Y.; Armes, S. P. RAFT Synthesis of Sterically Stabilized Methacrylic Nanolatexes and Vesicles by Aqueous Dispersion Polymerization. Angew. Chemie Int. Ed. **2010**, 49 (24), 4042–4046.

(85) Canning, S. L.; Smith, G. N.; Armes, S. P. A Critical Appraisal of RAFT-Mediated Polymerization-Induced Self-Assembly. Macromolecules **2016**, 49 (6), 1985–2001.

(86) Liu, C.; Hong, C. Y.; Pan, C. Y. Polymerization Techniques in Polymerization-Induced Self-Assembly (PISA). Polym. Chem. **2020**, 11 (22), 3673–3689.

(87) Wang, G.; Schmitt, M.; Wang, Z.; Lee, B.; Pan, X.; Fu, L.; Yan, J.; Li, S.; Xie, G.; Bockstaller, M. R.; Matyjaszewski, K. Polymerization-Induced Self-Assembly (PISA) Using ICAR ATRP at Low Catalyst Concentration. Macromolecules **2016**, 49 (22), 8605–8615.

(88) Sugihara, S.; Blanazs, A.; Armes, S. P.; Ryan, A. J.; Lewis, A. L. Aqueous Dispersion Polymerization: A New Paradigm for in Situ Block Copolymer Self-Assembly in Concentrated Solution. J. Am. Chem. Soc. **2011**, 133 (39), 15707–15713.

(89) Delaittre, G.; Dire, C.; Rieger, J.; Putaux, J. L.; Charleux, B. Formation of Polymer Vesicles by Simultaneous Chain Growth and Self-Assembly of Amphiphilic Block Copolymers. Chem. Commun. **2009**, No. 20, 2887–2889.

(90) Zhang, L.; Song, C.; Yu, J.; Yang, D.; Xie, M. One-Pot Synthesis of Polymeric Nanoparticle by Ring-Opening Metathesis Polymerization. J. Polym. Sci. Part A Polym. Chem. **2010**, 48 (22), 5231–5238.

(91) Liu, J.; Liao, Y.; He, X.; Yu, J.; Ding, L.; Xie, M. Facile One-Pot Approach for Preparing Functionalized Polymeric Nanoparticles via ROMP. Macromol. Chem. Phys. **2011**, 212 (1), 55–63.

(92) Foster, J. C.; pyridon Varlas, S.; Blackman, L. D.; Arkinstall, L. A.; OReilly, R. K.; DBlackman, D.; oster, D. C.; arlas, S. V; Arkinstall, L. A. Ring-Opening Metathesis Polymerization in Aqueous Media Using a Macroinitiator Approach. Angew. Chemie Int. Ed. **2018**, 57 (33), 10672–10676.

(93) Pei, Y.; Dharsana, N. C.; Van Hensbergen, J. A.; Burford, R. P.; Roth, P. J.; Lowe, A. B. RAFT Dispersion Polymerization of 3-Phenylpropyl Methacrylate with Poly[2-(Dimethylamino)Ethyl Methacrylate] Macro-CTAs in Ethanol and Associated

Thermoreversible Polymorphism. Soft Matter **2014**, 10 (31), 5787–5796.

(94) Canning, S. L.; Cunningham, V. J.; Ratcliffe, L. P. D.; Armes, S. P. Phenyl Acrylate Is a Versatile Monomer for the Synthesis of Acrylic Diblock Copolymer Nano-Objects: Via Polymerization-Induced Self-Assembly. Polym. Chem. **2017**, 8 (33), 4811–4821.

(95) Lowe, A. B. RAFT Alcoholic Dispersion Polymerization with Polymerization-Induced Self-Assembly. Polymer **2016**, 106, 161–181.

(96) Pei, Y.; Thurairajah, L.; Sugita, O. R.; Lowe, A. B. RAFT Dispersion Polymerization in Nonpolar Media: Polymerization of 3-Phenylpropyl Methacrylate in n -Tetradecane with Poly(Stearyl Methacrylate) Homopolymers as Macro Chain Transfer Agents. Macromolecules **2015**, 48 (1), 236–244.

(97) Ratcliffe, L. P. D.; McKenzie, B. E.; Le Bouëdec, G. M. D.; Williams, C. N.; Brown, S. L.; Armes, S. P. Polymerization-Induced Self-Assembly of All-Acrylic Diblock Copolymers via RAFT Dispersion Polymerization in Alkanes. Macromolecules **2015**, 48 (23), 8594–8607.

(98) Zhou, D.; Kuchel, R. P.; Dong, S.; Lucien, F. P.; Perrier, S.; Zetterlund, P. B.; Zhou, D.; Dong, S.; Lucien, F. P.; Zetterlund, P. B.; Kuchel, R. P.; Perrier, S. Polymerization-Induced Self-Assembly under Compressed CO2: Control of Morphology Using a CO2-Responsive MacroRAFT Agent. Macromol. Rapid Commun. **2019**, 40 (2), 1800335.

(99) Xu, A.; Lu, Q.; Huo, Z.; Ma, J.; Geng, B.; Azhar, U.; Zhang, L.; Zhang, S. Synthesis of Fluorinated Nanoparticles via RAFT Dispersion Polymerization-Induced Self-Assembly Using Fluorinated Macro-RAFT Agents in Supercritical Carbon Dioxide. RSC Adv. **2017**, 7 (81), 51612–51620.

(100) György, C.; Verity, C.; Neal, T. J.; Rymaruk, M. J.; Cornel, E. J.; Smith, T.; Growney, D. J.; Armes, S. P. RAFT Dispersion Polymerization of Methyl Methacrylate in Mineral Oil: High Glass Transition Temperature of the Core-Forming Block Constrains the Evolution of Copolymer Morphology. Macromolecules **2021**, 54 (20), 9496–9509.

(101) Blanazs, A.; Ryan, A. J.; Armes, S. P. Predictive Phase Diagrams for RAFT Aqueous Dispersion Polymerization: Effect of Block Copolymer Composition, Molecular Weight, and Copolymer Concentration. Macromolecules **2012**, 45 (12), 5099–5107.

(102) Blanazs, A.; Madsen, J.; Battaglia, G.; Ryan, A. J.; Armes, S. P. Mechanistic Insights for Block Copolymer Morphologies: How Do Worms Form Vesicles? J. Am. Chem. Soc. **2011**, 133 (41), 16581–16587.

(103) Wang, X.; An, Z.; Wang, X.; An, Z. New Insights into RAFT Dispersion Polymerization-Induced Self-Assembly: From Monomer Library, Morphological Control, and Stability to Driving Forces. Macromol. Rapid Commun. **2019**, 40 (2), 1800325.

(104) Charleux, B.; Delaittre, G.; Rieger, J.; D'Agosto, F. Polymerization-Induced Self-Assembly: From Soluble Macromolecules to Block Copolymer Nano-Objects in One Step. Macromolecules **2012**, 45 (17), 6753–6765.

(105) Boissé, S.; Rieger, J.; Pembouong, G.; Beaunier, P.; Charleux, B. Influence of the Stirring Speed and CaCl2 Concentration on the Nano-Object Morphologies Obtained via RAFT-Mediated Aqueous Emulsion Polymerization in the Presence of a Water-Soluble MacroRAFT Agent. J. Polym. Sci. Part A Polym. Chem. **2011**, 49 (15), 3346–

3354.

(106) Khor, S. Y.; Truong, N. P.; Quinn, J. F.; Whittaker, M. R.; Davis, T. P. Polymerization-Induced Self-Assembly: The Effect of End Group and Initiator Concentration on Morphology of Nanoparticles Prepared via RAFT Aqueous Emulsion Polymerization. ACS Macro Lett. **2017**, 6 (9), 1013–1019.

(107) Zhang, X.; Rieger, J.; Charleux, B. Effect of the Solvent Composition on the Morphology of Nano-Objects Synthesized via RAFT Polymerization of Benzyl Methacrylate in Dispersed Systems. Polym. Chem. **2012**, 3 (6), 1502–1509.

(108) Zhang, W.; D'Agosto, F.; Boyron, O.; Rieger, J.; Charleux, B. Toward a Better Understanding of the Parameters That Lead to the Formation of Nonspherical Polystyrene Particles via RAFT-Mediated One-Pot Aqueous Emulsion Polymerization. Macromolecules **2012**, 45 (10), 4075–4084.

(109) Kim, H. J.; Ishizuka, F.; Kuchel, R. P.; Chatani, S.; Niino, H.; Zetterlund, P. B. Synthesis of Low Glass Transition Temperature Worms Comprising a Poly(Styrene-Stat-n-Butyl Acrylate) Core Segment via Polymerization-Induced Self-Assembly in RAFT Aqueous Emulsion Polymerization. Polym. Chem. **2022**, 13,1719-1730.

(110) Sugihara, S.; Blanazs, A.; Armes, S. P.; Ryan, A. J.; Lewis, A. L. Aqueous Dispersion Polymerization: A New Paradigm for in Situ Block Copolymer Self-Assembly in Concentrated Solution. J. Am. Chem. Soc. **2011**, 133 (39), 15707–15713.

(111) Doncom, K.; Warren, N. J.; Armes, S. P. Polysulfobetaine-Based Diblock Copolymer Nano-Objects via Polymerization-Induced Self-Assembly. Polym. Chem. **2015**, 6 (41), 7264–7273.

(112) Semsarilar, M.; Ladmiral, V.; Blanazs, A.; Armes, S. P. Anionic Polyelectrolyte-Stabilized Nanoparticles via RAFT Aqueous Dispersion Polymerization. Langmuir **2012**, 28 (1), 914–922.

(113) Jones, E. R.; Semsarilar, M.; Blanazs, A.; Armes, S. P. Efficient Synthesis of Amine-Functional Diblock Copolymer Nanoparticles via RAFT Dispersion Polymerization of Benzyl Methacrylate in Alcoholic Media. Macromolecules **2012**, 45 (12), 5091–5098.

(114) Derry, M. J.; Fielding, L. A.; Armes, S. P. Polymerization-Induced Self-Assembly of Block Copolymer Nanoparticles via RAFT Non-Aqueous Dispersion Polymerization. Prog. Polym. Sci. **2016**, 52, 1–18.

(115) An, Z.; Shi, Q.; Tang, W.; Tsung, C. K.; Hawker, C. J.; Stucky, G. D. Facile RAFT Precipitation Polymerization for the Microwave-Assisted Synthesis of Well-Defined, Double Hydrophilic Block Copolymers and Nanostructured Hydrogels. J. Am. Chem. Soc. **2007**, 129 (46), 14493–14499.

(116) Shen, W.; Chang, Y.; Liu, G.; Wang, H.; Cao, A.; An, Z. Biocompatible, Antifouling, and Thermosensitive Core-Shell Nanogels Synthesized by RAFT Aqueous Dispersion Polymerization. Macromolecules **2011**, 44 (8), 2524–2530.

(117) Liu, G.; Qiu, Q.; Shen, W.; An, Z. Aqueous Dispersion Polymerization of 2-Methoxyethyl Acrylate for the Synthesis of Biocompatible Nanoparticles Using a Hydrophilic RAFT Polymer and a Redox Initiator. Macromolecules **2011**, 44 (13), 5237–5245.

(118) Zhou, W.; Qu, Q.; Xu, Y.; An, Z. Aqueous Polymerization-Induced Self-Assembly for the Synthesis of Ketone-Functionalized Nano-Objects with Low Polydispersity. ACS Macro Lett. **2015**, 4 (5), 495–499.

(119) Byard, S. J.; Williams, M.; McKenzie, B. E.; Blanazs, A.; Armes, S. P. Preparation and Cross-Linking of All-Acrylamide Diblock Copolymer Nano-Objects via Polymerization-Induced Self-Assembly in Aqueous Solution. Macromolecules **2017**, 50 (4), 1482–1493.

(120) Figg, C. A.; Carmean, R. N.; Bentz, K. C.; Mukherjee, S.; Savin, D. A.; Sumerlin, B. S. Tuning Hydrophobicity To Program Block Copolymer Assemblies from the Inside Out. Macromolecules **2017**, 50 (3), 935–943.

(121) Wang, X.; An, Z. New Insights into RAFT Dispersion Polymerization-Induced Self-Assembly: From Monomer Library, Morphological Control, and Stability to Driving Forces. Macromol. Rapid Commun. **2019**, 40 (2), 1800325.

(122) Wang, X.; Zhou, J.; Lv, X.; Zhang, B.; An, Z. Temperature-Induced Morphological Transitions of Poly(Dimethylacrylamide)-Poly(Diacetone Acrylamide) Block Copolymer Lamellae Synthesized via Aqueous Polymerization-Induced Self-Assembly. Macromolecules **2017**, 50 (18), 7222–7232.

(123) Mukherjee, S.; Bapat, A. P.; Hill, M. R.; Sumerlin, B. S. Oximes as Reversible Links in Polymer Chemistry: Dynamic Macromolecular Stars. Polym. Chem. **2014**, 5 (24), 6923–6931.

(124) Qu, Q.; Liu, G.; Lv, X.; Zhang, B.; An, Z. In Situ Cross-Linking of Vesicles in Polymerization-Induced Self-Assembly. ACS Macro Lett. **2016**, 5 (3), 316–320.

(125) Wang, X.; Figg, C. A.; Lv, X.; Yang, Y.; Sumerlin, B. S.; An, Z. Star Architecture Promoting Morphological Transitions during Polymerization-Induced Self-Assembly. ACS Macro Lett. **2017**, 6 (4), 337–342.

(126) Byard, S. J.; Blanazs, A.; Miller, J. F.; Armes, S. P. Cationic Sterically Stabilized Diblock Copolymer Nanoparticles Exhibit Exceptional Tolerance toward Added Salt. Langmuir **2019**, 35 (44), 14348–14357.

(127) Borisov, O. V.; Zhulina, E. B. Morphology of Micelles Formed by Diblock Copolymer with a Polyelectrolyte Block. Macromolecules **2003**, 36 (26), 10029–10036.

(128) Zhang, W.; D'Agosto, F.; Boyron, O.; Rieger, J.; Charleux, B. One-Pot Synthesis of Poly(Methacrylic Acid-Co-Poly(Ethylene Oxide) Methyl Ether Methacrylate)-b-Polystyrene Amphiphilic Block Copolymers and Their Self-Assemblies in Water via RAFT-Mediated Radical Emulsion Polymerization. A Kinetic Study. Macromolecules **2011**, 44 (19), 7584–7593.

(129) Boissé, S.; Rieger, J.; Belal, K.; Di-Cicco, A.; Beaunier, P.; Li, M. H.; Charleux, B. Amphiphilic Block Copolymer Nano-Fibers via RAFT-Mediated Polymerization in Aqueous Dispersed System. Chem. Commun. **2010**, 46 (11), 1950–1952.

(130) Zhang, X.; Boissé, S.; Zhang, W.; Beaunier, P.; D'Agosto, F.; Rieger, J.; Charleux, B. Well-Defined Amphiphilic Block Copolymers and Nano-Objects Formed in Situ via RAFT-Mediated Aqueous Emulsion Polymerization. Macromolecules **2011**, 44 (11), 4149–4158.

(131) Zhang, B.; Yan, X.; Alcouffe, P.; Charlot, A.; Fleury, E.; Bernard, J. Aqueous RAFT Polymerization of Imidazolium-Type Ionic Liquid Monomers: En Route to Poly(Ionic Liquid)-Based Nanoparticles through RAFT Polymerization-Induced Self-Assembly. ACS Macro Lett. **2015**, 4 (9), 1008–1011.

(132) Williams, M.; Penfold, N. J. W.; Armes, S. P. Cationic and Reactive Primary Amine-Stabilised Nanoparticles via RAFT Aqueous Dispersion Polymerisation. Polym.

Chem. **2016**, 7 (2), 384–393.

(133) Williams, M.; Penfold, N. J. W.; Lovett, J. R.; Warren, N. J.; Douglas, C. W. I.; Doroshenko, N.; Verstraete, P.; Smets, J.; Armes, S. P. Bespoke Cationic Nano-Objects: Via RAFT Aqueous Dispersion Polymerisation. Polym. Chem. **2016**, 7 (23), 3864–3873.

(134) Semsarilar, M.; Ladmiral, V.; Blanazs, A.; Armes, S. P. Cationic Polyelectrolyte-Stabilized Nanoparticles via RAFT Aqueous Dispersion Polymerization. Langmuir **2013**, 29 (24), 7416–7424.

(135) Zhou, D.; Dong, S.; Kuchel, R. P.; Perrier, S.; Zetterlund, P. B. Polymerization Induced Self-Assembly: Tuning of Morphology Using Ionic Strength and PH. Polym. Chem. **2017**, 8 (20), 3082–3089.

(136) Blanazs, A.; Verber, R.; Mykhaylyk, O. O.; Ryan, A. J.; Heath, J. Z.; Douglas, C. W. I.; Armes, S. P. Sterilizable Gels from Thermoresponsive Block Copolymer Worms. J. Am. Chem. Soc. **2012**, 134 (23), 9741–9748.

(137) Lovett, J. R.; Warren, N. J.; Armes, S. P.; Smallridge, M. J.; Cracknell, R. B. Order-Order Morphological Transitions for Dual Stimulus Responsive Diblock Copolymer Vesicles. Macromolecules **2016**, 49 (3), 1016–1025.

(138) Penfold, N. J. W.; Whatley, J. R.; Armes, S. P. Thermoreversible Block Copolymer Worm Gels Using Binary Mixtures of PEG Stabilizer Blocks. Macromolecules **2019**, 52 (4), 1653–1662.

(139) Beattie, D. L.; Mykhaylyk, O. O.; Ryan, A. J.; Armes, S. P. Rational Synthesis of Novel Biocompatible Thermoresponsive Block Copolymer Worm Gels. Soft Matter **2021**, 17 (22), 5602–5612.

(140) Verber, R.; Blanazs, A.; Armes, S. P. Rheological Studies of Thermo-Responsive Diblock Copolymer Worm Gels. Soft Matter **2012**, 8 (38), 9915–9922.

(141) Pei, Y.; Lowe, A. B.; Roth, P. J.; Pei, Y.; Roth, P. J.; Lowe, A. B. Stimulus-Responsive Nanoparticles and Associated (Reversible) Polymorphism via Polymerization Induced Self-Assembly (PISA). Macromol. Rapid Commun. **2017**, 38 (1), 1600528.

(142) Ratcliffe, L. P. D.; Derry, M. J.; Ianiro, A.; Tuinier, R.; Armes, S. P. A Single Thermoresponsive Diblock Copolymer Can Form Spheres, Worms or Vesicles in Aqueous Solution. Angew. Chemie **2019**, 131 (52), 19140–19146.

(143) Penfold, N. J. W.; Lovett, J. R.; Warren, N. J.; Verstraete, P.; Smets, J.; Armes, S. P. PH-Responsive Non-Ionic Diblock Copolymers: Protonation of a Morpholine End-Group Induces an Order-Order Transition. Polym. Chem. **2016**, 7 (1), 79–88.

(144) Penfold, N. J. W.; Lovett, J. R.; Verstraete, P.; Smets, J.; Armes, S. P. Stimulus-Responsive Non-Ionic Diblock Copolymers: Protonation of a Tertiary Amine End-Group Induces Vesicle-to-Worm or Vesicle-to-Sphere Transitions. Polym. Chem. **2016**, 8 (1), 272–282.

(145) Dorsman, I. R.; Derry, M. J.; Cunningham, V. J.; Brown, S. L.; Williams, C. N.; Armes, S. P. Tuning the Vesicle-to-Worm Transition for Thermoresponsive Block Copolymer Vesicles Prepared via Polymerisation-Induced Self-Assembly. Polym. Chem. **2021**, 12 (9), 1224–1235.

(146) Derry, M. J.; Mykhaylyk, O. O.; Armes, S. P. A Vesicle-to-Worm Transition Provides a New High-Temperature Oil Thickening Mechanism. Angew. Chemie **2017**, 129 (7), 1772–1776.

(147) Nizardo, N.; Schanzenbach, D.; Schönemann, E.; Laschewsky, A.; Nizardo, N. M.; Schanzenbach, D.; Schönemann, E.; Laschewsky, A. Exploring Poly(Ethylene Glycol)-Polyzwitterion Diblock Copolymers as Biocompatible Smart Macrosurfactants Featuring UCST-Phase Behavior in Normal Saline Solution. Polymers **2018**, 10 (3), 325.

(148) Andersson, T.; Holappa, S.; Aseyev, V.; Tenhu, H. Complexation of Linear and Poly(Ethylene Oxide)-Grafted Poly(Methacryl Oxyethyl Trimethylammonium Chloride) with Poly(Ethylene Oxide-Block-Sodium Methacrylate). J. Polym. Sci. Part A Polym. Chem. **2003**, 41 (13), 1904–1914.

(149) Cong, Y.; Zhou, Q.; Chen, B.; Fang, J.; Fu, J. Morphological Transformations of Nonequilibrium Assemblies of Amphiphilic Diblock Copolymer. Colloid J. **2014**, 76 (6), 774–781.

(150) Warren, N. J.; Mykhaylyk, O. O.; Ryan, A. J.; Williams, M.; Doussineau, T.; Dugourd, P.; Antoine, R.; Portale, G.; Armes, S. P. Testing the Vesicular Morphology to Destruction: Birth and Death of Diblock Copolymer Vesicles Prepared via Polymerization-Induced Self-Assembly. J. Am. Chem. Soc. **2015**, 137 (5), 1929–1937.

(151) Siirilä, J.; Häkkinen, S.; Tenhu, H. The Emulsion Polymerization Induced Self-Assembly of a Thermoresponsive Polymer Poly(N-Vinylcaprolactam). Polym. Chem. **2019**, 10 (6), 766–775.

(152) Zhang, Q.; Zeng, R.; Zhang, Y.; Chen, Y.; Zhang, L.; Tan, J. Two Polymersome Evolution Pathways in One Polymerization-Induced Self-Assembly (PISA) System. Macromolecules **2020**, 53 (20), 8982–8991.

(153) Doncom, K. E. B.; Warren, N. J.; Armes, S. P. Polysulfobetaine-Based Diblock Copolymer Nano-Objects via Polymerization-Induced Self-Assembly. Polym. Chem. **2015**, 6 (41), 7264–7273.

(154) Ratcliffe, L. P. D.; Derry, M. J.; Ianiro, A.; Tuinier, R.; Armes, S. P. A Single Thermoresponsive Diblock Copolymer Can Form Spheres, Worms or Vesicles in Aqueous Solution. Angew. Chemie - Int. Ed. **2019**, 58 (52), 18964–18970.

(155) Hahn, L.; Maier, M.; Stahlhut, P.; Beudert, M.; Flegler, V.; Forster, S.; Altmann, A.; Töppke, F.; Fischer,K.; Seiffert, S.; Böttcher, B.; Lühmann, T.; Luxenhofer, R. Inverse Thermogelation of Aqueous Triblock Copolymer Solutions into Macroporous Shear-Thinning 3D Printable Inks. ACS Appl. Mater. Interfaces **2020**, 12 (11), 12445–12456.